Vol. 745: 73–94, 2024
https://doi.org/10.3354/meps14675

MARINE ECOLOGY PROGRESS SERIES
Mar Ecol Prog Ser

Published September 19

Model estimation of eastern oyster larval performance from food quantity and quality measures in western Mississippi Sound

James C. Klein[1,5,*], Eric N. Powell[1], Danielle A. Kreeger[2], Xiaodong Zhang[3], Sara M. Pace[4], Kelsey M. Kuykendall[1], Roger L. Thomas[2]

[1]Division of Coastal Sciences, The University of Southern Mississippi, Ocean Springs, MS 39564, USA
[2]The Academy of Natural Sciences of Drexel University, Philadelphia, PA 19103, USA
[3]Division of Marine Science, The University of Southern Mississippi, Stennis Space Center, MS 39556, USA
[4]North Carolina Department of Environmental Quality, Division of Marine Fisheries, Morehead City, NC 28557, USA
[5]*Present address:* Mississippi Department of Marine Resources, Office of Marine Fisheries, Biloxi, MS 39530, USA

ABSTRACT: Oyster *Crassostrea virginica* population recovery is critical in degraded estuarine systems, such as Mississippi Sound, USA, where repeated mass mortality events have depleted local oyster stocks. Owing to multiple recent die-offs, the western Mississippi Sound oyster population is recruitment-limited; population growth is constrained by the entry of new individuals into the extant population. Therefore, oyster recovery requires an adequate supply of larvae capable of timely development, growth, and successful metamorphosis. Larval performance and settlement potential are influenced by ambient temperature, salinity, and food supply. Food quantity is important to larvae, but so is food quality, as larvae require a balanced diet of lipids, proteins, and carbohydrates to develop and survive through metamorphosis. In this study, *in situ* environmental and food conditions during the 2021 and 2022 spawning seasons from 7 oyster reefs in western Mississippi Sound were integrated into an established biochemically based larval performance model to estimate periods facilitative of successful metamorphosis. In 2021, model-estimated larval survivorship was suppressed through much of the spawning season by prolonged, extremely low salinity (<5 ppt) and inadequately balanced food supply. Higher seasonal salinity and more balanced food composition increased model-estimated larval survivorship in 2022, despite lower total food content, suggesting larval performance was primarily governed by the quality of available food. Model-estimated settlement windows were compared to settlement windows derived from concomitant field observations of recruitment. Strong agreement between model-estimated and observed settlement windows validates the effectiveness of the model and informs on the underlying causes of recruitment limitation in western Mississippi Sound.

KEY WORDS: *Crassostrea virginica* · Larval development · Food quality · Modeling · Recruitment limitation

1. INTRODUCTION

Eastern oysters *Crassostrea virginica* are invaluable to North American East Coast and Gulf of Mexico estuaries (Harding & Mann 2001, Coen et al. 2007, Fulford et al. 2010, Grabowski et al. 2012, zu Ermgassen et al. 2013, Fodrie et al. 2017, La Peyre et al. 2019). The US Gulf of Mexico currently dominates commercial oyster landings after historic East Coast population collapses, most notably in Chesapeake Bay (Rothschild et al. 1994, MacKenzie 2007, Mann & Powell 2007). Gulf Coast populations are also not immune to global declining trends (Beck et al. 2011, Grabowski et al. 2017, Powers et al. 2017, Gledhill et al. 2020, Hesterberg et al. 2020, Pace et al. 2020a,b, Soniat et al. 2021). Particularly, the oyster population

*Corresponding author: james.klein@dmr.ms.gov

in western Mississippi Sound has been decimated (Gledhill et al. 2020, Pace et al. 2020a) to such a degree that no commercial harvesting has been permitted since 2018.

Mass mortality events have repeatedly plagued oysters in Mississippi Sound over the last century (e.g. Butler 1952, Gunter 1953a,b, MacKenzie 1977, Turner 2006, Brammer et al. 2007, Grabowski et al. 2017, Pace et al. 2020b, Pruett et al. 2024), most recently caused by freshwater diversions into the Bonnet Carré Spillway in 2019 (Gledhill et al. 2020, Pace et al. 2020a). The Bonnet Carré Spillway (built to divert Mississippi River floodwater away from the New Orleans area and into Mississippi Sound by way of Lake Pontchartrain; Lane et al. 2001, Parra et al. 2020) was opened twice in 2019, releasing freshwater for a total of 123 d (Gledhill et al. 2020). Consequently, western Mississippi Sound salinity remained at <5 ppt for multiple months, killing >90% of the already diminished oyster population (Gledhill et al. 2020, Pace et al. 2020a).

Adult oysters can tolerate salinities between 5 and 40 ppt and withstand extremely low salinities (<5 ppt) for short periods (Galtsoff 1964, Shumway 1996, McFarland et al. 2022), but prolonged exposure to oligohaline conditions can trigger mass mortality events (Gunter 1953a, Andrews et al. 1959, Pollack et al. 2011, La Peyre et al. 2013, Munroe et al. 2013, Powers et al. 2017, Gledhill et al. 2020, Du et al. 2021). Prompt recovery from mass mortality events is plausible (Gunter 1953b, Livingston et al. 1999, Pollack et al. 2011, La Peyre et al. 2013, Pace et al. 2020a), especially for Gulf Coast oyster populations characterized by multiple spawns per season (Ingle 1951, Hopkins 1954, Hayes & Menzel 1981) and relatively rapid, continuous growth (Butler 1952, Ingle & Dawson 1952, Hofmann et al. 1992). Conversely, factors impeding population recovery include poor recruitment, often as a result of inadequate substrate and post-settlement survival, typically limited by crab, drill, and/or turbellarian predation (Provenzano 1961, Osman et al. 1989, Barnes et al. 2010, Knights & Walters 2010, De Santiago et al. 2019, Morgan & Rakocinski 2022). Loss of adults during mass mortalities poses the dual challenge of substrate limitation and recruitment limitation (Brumbaugh & Coen 2009, Pace et al. 2023), particularly for degraded populations, as is the case in western Mississippi Sound (Morgan & Rakocinski 2022).

Since the 2019 Bonnet Carré Spillway mass mortality event, however, low salinity regimes and insufficient larval supply appear to have shifted the predominant control on oyster population recovery to recruitment limitation (Morgan & Rakocinski 2022), possibly due to inadequate larval supply by limited broodstock or by poor larval performance (Brumbaugh & Coen 2009). Although taphonomic processes that remove suitable substrate from extant oyster beds remain an obstacle to population recovery (Pace et al. 2020b, 2023), poor settlement to existing substrates following the 2019 mass mortality indicates that recruitment potential may also be a primary limitation (Morgan & Rakocinski 2022, Pace et al. 2023).

Successful larval recruitment to populations is a primary requisite for population recovery, growth, and maintenance but depends on an abundant and competent larval supply, among other factors (Coen & Luckenbach 2000, Lipcius et al. 2015, Powell et al. 2018, Hemeon et al. 2020, Morgan & Rakocinski 2022, Solinger et al. 2022, Pace et al. 2023). Numerous factors control larval performance, through constraints on fertilization success, growth and development, and successful metamorphosis, and through variability in physiologic condition and environmental stressors, such as temperature, salinity, and food supply (Loosanoff & Davis 1963, Dekshenieks et al. 1993, Bochenek et al. 2001, Powell et al. 2002, 2004, Hofmann et al. 2004, Klein et al. 2023). Being more limited in environmental ambit than their eurytopic adult counterparts, oyster larvae tolerate narrower temperature–salinity ranges (Shumway 1996, McFarland et al. 2022). Eastern oyster larval growth is optimal between 27° and 32°C and marginal above 35° or below 17.5°C (Davis & Calabrese 1964, Dekshenieks et al. 1993). For salinity, larvae exhibit no growth below 5 ppt, minimal growth below 7.5 ppt, and maximal growth between 17.5 and 25 ppt for most temperatures (Davis 1958, Dekshenieks et al. 1993). Geographic variation and parentage, however, also influence larval tolerances (Shumway 1996, Eierman & Hare 2013, Scharping et al. 2019).

Food availability and its nutritional balance also govern oyster larval performance (Wikfors et al. 1984, Soniat & Ray 1985, Berg & Newell 1986, Utting 1986, Thompson & Harrison 1992, Baldwin & Newell 1995a, Wilson-Ormond et al. 1997). Dekshenieks et al. (1993) suggested food concentrations exceeding 3 mg l^{-1} maximize larval success, whereby performance and survival decline when food content declines below 2 mg l^{-1} (Rhodes & Landers 1973, Bochenek et al. 2001, Powell et al. 2002, 2004, Hofmann et al. 2004). Larval success also depends on proper food quality, or an appropriate balance of lipids, proteins, and carbohydrates (e.g. Wikfors et al. 1984, Thompson & Harrison 1992, Thompson et al. 1996, Hendriks et al. 2003, Przeslawski et al. 2008, Zhang et al. 2010,

Matias et al. 2015, Da Costa et al. 2016). Biochemically balanced diets ensure both timely somatic growth and accumulation of adequate energy stores for development and metamorphosis (Bochenek et al. 2001, Powell et al. 2002, 2004, Hofmann et al. 2004, Klein et al. 2023). Oyster larvae feed on a range of particles varying in size and composition not limited to phytoplankton (Baldwin & Newell 1991, 1995a,b), and therefore evaluating food by its compositional assemblage of lipid, protein, and carbohydrate surpasses other metrics such as chlorophyll, total organic carbon, and total seston (Soniat et al. 1984, 1998, Soniat & Ray 1985, Berg & Newell 1986).

Modeling larval performance offers the most time- and cost-effective approach to investigate the response of larvae to various external environmental and biological conditions. To effectively estimate larval performance and metamorphic success, these modeling efforts must incorporate food supply (both quantity and quality) and physiological variation alongside other key environmental parameters such as temperature and salinity (Bochenek et al. 2001, Fach et al. 2002, Powell et al. 2002, 2004, Hofmann et al. 2004, Pfeiffer-Hoyt & McManus 2005, Klein et al. 2023). One such larval model was originally developed for the Pacific oyster *C. gigas* (Bochenek et al. 2001, Powell et al. 2002, 2004, Hofmann et al. 2004) and later modified for *C. virginica* (Klein et al. 2023). The model is biochemically based, characterizing both larvae and food by lipid, protein, and carbohydrate (LPC) content. In the model, food supply, temperature, and salinity collaboratively govern larval growth, development, and ultimately success at metamorphosis. Additionally, physiological variations in assimilation efficiency and egg quality (via initial size and lipid content) influence larval performance and survivorship. This model accurately predicted larval performance under theoretical hatchery conditions (Bochenek et al. 2001, Powell et al. 2002, 2004, Hofmann et al. 2004), but more recent work has also verified that model-estimated oyster settlement periods conform to observed recruitment patterns in Delaware Bay from 2009 to 2011 (Klein et al. 2023).

The current study utilizes the modified *C. virginica* larval performance model to better understand how exogenous conditions influence larval development and success at settlement, which ultimately contribute to effective population maintenance and growth. Using Mississippi Sound conditions as a case study, the model is employed to evaluate the influence of environmental and biological conditions on recruitment potential in the oyster population. The larval model simulated conditions present in western Mississippi Sound during the 2021 and 2022 spawning seasons (May through October) using *in situ* temperature, salinity, and food supply measurements to estimate larval survival and settlement potential. Furthermore, model-predicted settlement windows from 2022 were compared to concurrent field recruitment observations to validate model output. Verified model results provided insight into the factors limiting local recruitment and inhibiting population recovery from recent mass mortality events. More broadly, the model offers direct, observation-based evidence on the importance of food supply for successful larval development and, ultimately, the establishment of new individuals into populations.

2. MATERIALS AND METHODS

2.1. Site description

Mississippi Sound (Fig. 1) is a well-mixed estuary with an average mean-low-water depth of 3 m (Eleuterius 1978). It can be divided into 3 sections based on distinctive hydrologic characteristics (Eleuterius 1976). The western portion, which contains most of the commercially important oyster *Crassostrea virginica* beds within the estuarine system (Eleuterius 1977, MacKenzie 1977), extends from Cat Island to Half Moon Island. Western Mississippi Sound is characterized by strong vertical mixing, high turbidity, minimal temperature variation, and lower salinity compared to the central and eastern counterparts due to restricted saltwater exchange (Eleuterius 1976 and references therein). Freshwater primarily enters western Mississippi Sound through St. Joe Pass via Pearl River outflow but also through St. Louis Bay (Eleuterius 1976). Brackish water from Chandeleur Sound, Louisiana, enters through Cat Island Pass, while saltwater is exchanged via Ship Island Pass on the eastern side of Cat Island (Eleuterius 1976). Consequently, western Mississippi Sound exhibits a decreasing east-to-west salinity gradient governed by freshwater inflow, whereby periods of high river discharge depress salinities eastward, beyond Pass Christian Reef (Eleuterius 1976, 1977). Seven established oyster beds from western Mississippi Sound were selected for this case study (Fig. 1).

2.2. Modeling larval performance

This study relies on a larval performance model designed to evaluate the response of a range of unique

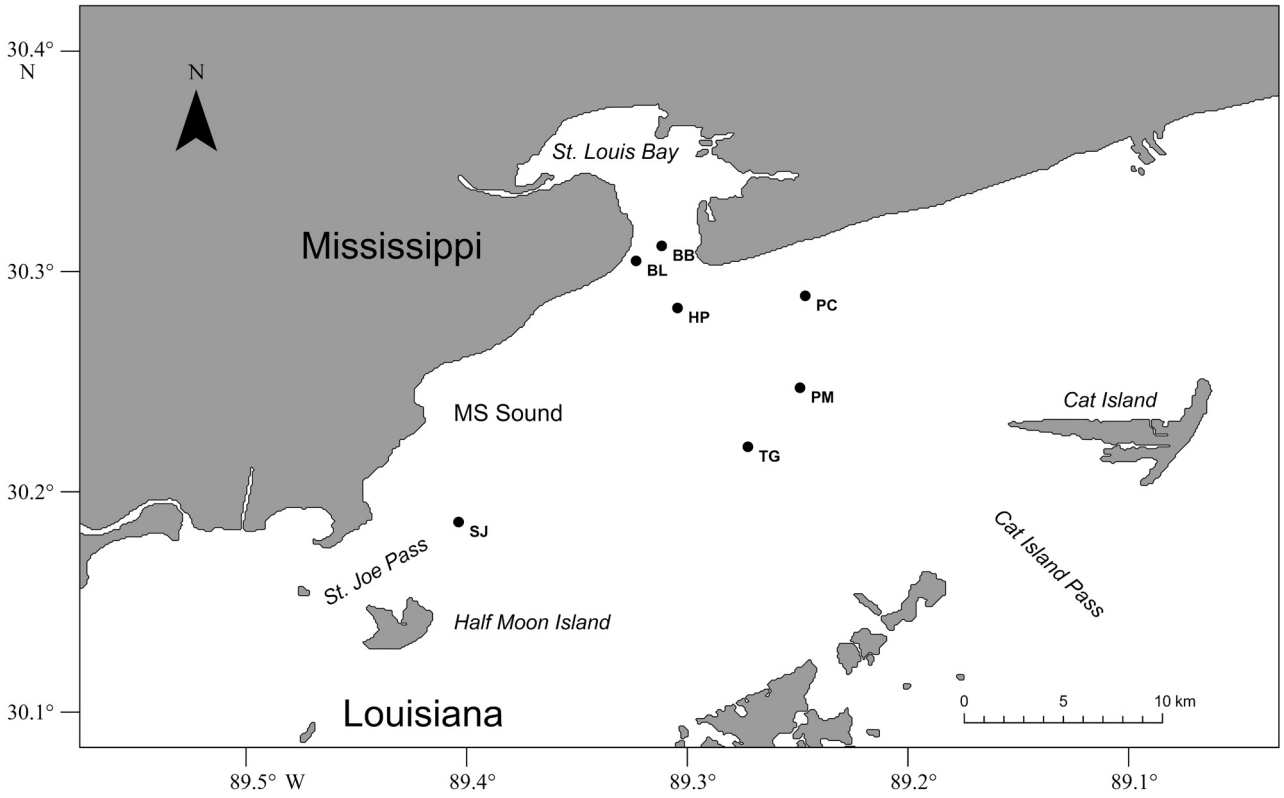

Fig. 1. Western Mississippi Sound and sample sites. PC: Pass Christian; PM: Pass Marianne; TG: Telegraph; SJ: St. Joe; HP: Henderson Point; BL: Bay St. Louis; BB: Between Bridges

larval phenotypes to ambient environmental and food conditions. Field-collected data served as model input. Temperature and salinity were measured *in situ* to parameterize modeled environmental conditions (Section 2.2.1). Water samples were concurrently collected to provide food quantity and quality metrics (Section 2.2.2). Model structure and subsequent adaptations were extensively detailed in Bochenek et al. (2001), Powell et al. (2002, 2004), Hofmann et al. (2004), and Klein et al. (2023) and are briefly summarized herein (Section 2.2.3). Model output includes larval survivorship and estimated settlement windows, which portray durations conducive to successful larval development and settlement in response to observed exogenous conditions (Section 2.2.4). Finally, model-estimated settlement windows from 2022 were compared to concurrent recruitment observations to provide model validation (Section 2.3).

2.2.1. Environmental conditions

Water sampling occurred from May through October of 2021 and 2022, as close to biweekly as possible, encapsulating the entire historical Gulf of Mexico spawning season (Ogle 1979, Hayes & Menzel 1981). Temperature and salinity were measured by an SBE-49 FastCAT CTD Sensor (Sea-Bird Scientific) just above each selected oyster bed (Fig. 1), and each recorded measurement was the median calculated from an approximately 10 min observation period.

2.2.2. Biochemical food metrics

Water samples from each site (Fig. 1) were collected approximately 0.33 m below the surface into 3 l carboys and stored on ice until laboratory processing as described by Powell et al. (2012). Samples were pre-filtered through a 105 µm sieve to exclude large particles and then vacuum-filtered onto pre-combusted 47 mm Whatman-type glass fiber filters (0.3 µm post-combustion retention threshold) at 90% clogging volume (between 90 and 600 ml) to maximize sample volume but avoid blockage. Three filters were processed from the same water sample for separate lipid, protein, and labile carbohydrate content analyses and stored frozen until analysis. Biochemical analyses were conducted using established methods adapted from Kreeger et al. (1997) and Powell et al. (2012) and

most recently employed by Klein et al. (2023) to quantify food supply in larval performance modeling efforts.

Total food quantity (expressed as LPC) was calculated as the sum of each biochemical constituent. The proportion of each individual biochemical constituent to LPC defined food quality. Food supply metrics, referring to both food quantity and quality, were input into the larval performance model. The protein-to-(lipid+carbohydrate) ratio (P:LC) was calculated to evaluate the relative proportion of protein (primarily utilized by larvae for somatic growth) to constituents mainly associated with energy expenditure and storage (Klein et al. 2023).

Biochemical measures included all particles ranging from approximately 0.3 to 105 µm. Although larger larvae are capable of feeding on particles >30 µm, most ingested food ranges between 0.5 and 12 µm (Baldwin & Newell 1995b). Thus, the food supply measured in this study encompassed a range of food sizes larger than the preferential larval food size but remains consistent with previous measures of food quantity and quality for comparison (e.g. Powell et al. 2012).

2.2.3. Larval performance model structure

The model used in this study is biochemically based and has been previously utilized to simulate larval growth, development, and metamorphosis in *C. gigas* (Bochenek et al. 2001, Powell et al. 2002, 2004, Hofmann et al. 2004) and *C. virginica* (Klein et al. 2023). Model equations are provided in Bochenek et al. (2001) and Klein et al. (2023), but briefly, the model uses parameters for the known biochemical composition, respiration, and filtration rates of larvae as well as population dynamics to simulate their growth and development at varying environmental conditions.

The model simulated a 40 d time period, almost twice the duration of commonly observed oyster larval lifespans (Prytherch 1929, Nelson 1955, Dekshenieks et al. 1993, Ben Kheder et al. 2010, Brunner et al. 2016, McDonald et al. 2023), to provide sufficient time for simulated larvae to complete all larval stages, if viable. To reflect observed environmental variability, each simulation comprised temperature, salinity, and food supply observations from 3 sequential sample dates. The first date established conditions at the egg hatch date (Day 0), while the latter 2 configured conditions for subsequent days corresponding to the respective sample intervals. Conditions were linearly interpolated between defined observations.

Physiological variation in growth efficiency (via assimilation efficiency) and in initial egg quality (via initial egg size and maternal lipid content) were incorporated into the model to represent observed variation in bivalve larval cohorts (Kraeuter et al. 1981, Hendriks et al. 2003, Langdon et al. 2003, Phillips 2007, Powell et al. 2011). Accordingly, each simulation case generated 816 larvae with distinct phenotypic variations in assimilation efficiency, initial egg size, and initial lipid content. Assimilation efficiency ranged between 0.55 and 0.90. Assimilation efficiencies are poorly known for larvae, but a somewhat wider range is recorded for adults (Hall et al. 2020). Initial egg diameter varied between 48 and 66 µm, a range within observed *C. virginica* egg diameters (Gallager & Mann 1986a, Kennedy et al. 1995, Powell et al. 2011). Maternal lipid content was determined by initial egg diameter and an initial lipid multiplier (Klein et al. 2023), ranging between 50 and 150% of the presumed mean maternal lipid content. The initial lipid content calculations were constructed based on *C. virginica* larval size and lipid content observations by Gallager et al. (1986) and Gallager & Mann (1986a,b). Phenotypes with 64 µm initial egg diameters and initial lipid multipliers $\geqslant$1.3 or 66 µm diameters and multipliers $\geqslant$1.1 were excluded from simulations, as their phenotypic combinations yielded incompatible configurations for egg biochemical stores (Klein et al. 2023). Limited knowledge of within-cohort phenotypic variability required that all simulated phenotypic variations be weighted equally (Klein et al. 2023).

The influence of temperature and salinity on simulated larvae followed Dekshenieks et al. (1993), whereby *C. virginica* larvae do not grow or feed at salinities of $\leqslant$5 ppt regardless of temperature. Growth is limited at salinities between 5 and 7.5 ppt at all temperatures (Dekshenieks et al. 1993). Simulated larvae do not die immediately from low-salinity exposure, but reduced feeding and longer development times impose greater energetic stresses on larvae, leading to lower metamorphic success (Klein et al. 2023).

Each biochemical constituent has a distinct role in larval development, so the availability of lipids, proteins, and carbohydrates synergistically affects growth and survival through settlement in the model. First, lipid content was evenly divided between polar and neutral lipids in the model (Klein et al. 2023). Assimilated protein, polar lipid, and carbohydrate each accumulate into their respective structural pools and contribute to somatic growth. Assimilated carbohydrate also covers respiratory demands, although

other constituents can mobilize if carbohydrate stores are insufficient. All biochemical constituents but protein are interconvertible if another constituent is depleted. Excess assimilated polar lipid and carbohydrate can transfer to the neutral lipid reserve, of which the primary purpose is energy storage for metamorphosis. Proper ratios of somatic polar lipid (0.11) and carbohydrate (0.01) to protein must be maintained for survival (Bochenek et al. 2001); otherwise, structural imbalances induce mortality in the model. Additionally, the protein-to-ash (inorganic material) ratio must be maintained above the lower critical threshold (0.7) to avoid starvation death. Consistent with the known ability of oyster larvae to withstand starvation stress (His & Seaman 1992, Moran & Manahan 2004, McFarland et al. 2020), starvation leading to a reduction in condition above this threshold is permitted but limits growth until the deficit is repaired.

Metamorphic competency requires larvae to reach ⩾275 µm in length and withstand a 25% neutral lipid reduction within 1 d. The neutral lipid reduction results from lowered filtration rates once larvae exceed 250 µm, as pediveligers rely more on stored energy (Bochenek et al. 2001). If metamorphic competency requisites were not satisfied before simulation Day 40, larvae were assumed to die by predation or be dispersed out of their habitat (Dekshenieks et al. 1997). Larvae immediately attempt metamorphosis once competent and are successful if their neutral lipid pool is greater than their somatic polar lipid pool post-competency. This theoretical hurdle was imposed by Bochenek et al. (2001) and corroborated by Klein et al. (2023), as details of the metamorphic process are poorly known.

2.2.4. Model output

For each simulation, the percentage of phenotypes to successfully metamorphose defined survivorship. Although survivorship herein does not reflect the number of larvae that are anticipated to survive in the field, as cohort sizes are unknown, it represents the likelihood of survival for larvae over an expected phenotypic range given observed exogenous conditions. Model-estimated survivorship cannot be compared directly to observed recruitment, as spawning times and spawning output are unknown. However, survivorship can be used as an index to evaluate the favorability of environmental conditions and food supply during periods of the spawning season.

Additionally, the model predicted planktonic larval durations (PLDs) for each viable phenotype, which were used to derive site-specific settlement windows. Model-estimated settlement windows were defined as the period between the earliest and latest successful metamorphosis attempt at each site. For analyses herein, the central 80th percentile period in which viable larvae metamorphosed established model-estimated settlement windows specific to each site.

2.3. Observed recruitment and model verification

Oyster monitoring surveys occurred at 5 sites monthly from May through December 2022 (Fig. 1). Early December sampling substituted for November observations. St. Joe was inaccessible during July and December surveys. Pass Marianne and Telegraph were also inaccessible in December. Survey protocols were described by Pace et al. (2020b). Up to 1.5 standard commercial bushels of oyster bed material (i.e. live individuals, boxes, cultch), or less, depending on reef condition, were collected using a standard commercial oyster dredge. Spat, defined as individuals ⩽25 mm in shell length, were counted and measured, although some new recruits may have exceeded the 25 mm threshold, given the rapid growth rates commonly observed in the Gulf of Mexico (Hayes & Menzel 1981). Recruitment was standardized to the number of spat per gram carbonate in the analyzed sample for comparison between reefs.

Calculations of observed recruitment-derived settlement windows were modified from Klein et al. (2023). First, the approximate number of days post-settlement for each individual was calculated as the difference in observed spat shell length and median modeled length at settlement (0.35 mm), divided by a uniform northern Gulf of Mexico spat growth rate (0.79 mm d^{-1}; Hayes & Menzel 1981). Individual settlement dates were then back-calculated from their respective observation date by the approximate days post-settlement. The central 80th percentile range of individual settlement dates from all sites defined the comprehensive observed settlement window.

Hayes & Menzel (1981) offer the only published northern Gulf of Mexico spat growth rates known to the authors, reporting a faster spat growth rate from one estuary (0.79 mm d^{-1}) than another (0.45 mm d^{-1}). The faster growth rate was used for calculating observed settlement windows in the current study because the latter produced infeasible estimates of western Mississippi Sound recruitment, as early as February (Pace et al. 2020b). Similar to adult oyster

growth in the northern Gulf of Mexico (Ingle & Dawson 1952, Butler 1953, Kraeuter et al. 2007), observed spat growth rates are more rapid than those in northern latitudes (Nelson 1917, Dunn et al. 2014, Munroe et al. 2017). A caveat of utilizing an undeviating rate is that it ignores spatiotemporal variation in individual growth due to site-specific environmental and food conditions at different times of the spawning season (Flores-Vergara et al. 2004, Dunn et al. 2014, Munroe et al. 2017, Manuel et al. 2023). Information is insufficient to account for such details in Mississippi Sound.

The duration and timing of observed settlement windows were then compared to model-estimated settlement windows, serving to validate the ability of the model to predict periods of favorable environmental and food conditions facilitative of larval survival and survivorship. This verification method was first employed by Klein et al. (2023) and successfully validated the model for Delaware Bay.

2.4. Statistical analysis

All statistical analyses were conducted with R v.4.2.3 (R Core Team 2023) in RStudio. Type III ANOVAs and ANCOVAs were executed using the 'car' package (Fox & Weisberg 2019), and least-squares (LS) mean pairwise analyses were performed using the 'emmeans' package (Lenth 2023). The effects of year and site on salinity and temperature were evaluated to identify potential causes of variation in larval performance. Interaction terms that were not significant ($\alpha > 0.05$) were removed from all ANOVA and ANCOVA models. Additionally, separate ANCOVAs were run on lipid, protein, carbohydrate, LPC, and the P:LC ratio using year, temperature, and salinity as main effects. Site was not a significant effect in any model and thus was removed. Statistical results presented were obtained using parametric ANOVAs on untransformed data. Although ANOVAs are robust to distributional effects (Schmider et al. 2010), the influence of variations in distribution and homogeneity was checked by comparing the results of parametric ANOVAs to ANOVAs using ranked data. As expected, results were identical in identifying significance at $\alpha = 0.05$.

Given the high occurrence in 2021 of cases in which all larval phenotypes were non-viable, a binomial test rather than ANOVA was used to examine whether the observed probability of a viable simulation case (survivorship > 0%) in 2021 was significantly different from what was expected based on the probability observed for a 2022 case. Additionally, ANOVAs were used to evaluate the effects of site and year on modeled PLD and final length at metamorphosis. Furthermore, the effect of site on PLD and final length was evaluated on viable larvae from each year separately.

3. RESULTS

3.1. Observed environmental and food conditions

Observed temperature ranged between 20 and 32°C during both oyster *Crassostrea virginica* spawning seasons and exhibited minimal variation across sites (Fig. 2A). The effect of site was not significant for temperature, although year was (Table 1). The average (±SD) temperature in 2021 (26.4 ± 2.6°C) was lower than in 2022 (28.0 ± 3.0°C). Across both years, salinity reached an initial peak between late July and mid-August, followed by a decline through September and a secondary peak beginning in October (Fig. 2B). Observed salinity varied significantly across both site and year (Table 1). Abnormally high annual precipitation and severe weather in 2021 caused the average (±SD) salinity (5.0 ± 4.4 ppt) to be lower than in 2022 (13.6 ± 5.2 ppt). Through both spawning seasons, observed salinity at Between Bridges, Bay St. Louis, and St. Joe were significantly different from Telegraph and Pass Marianne (Table 2). Observed salinity from Henderson Point and Pass Christian were not significantly different from any other location (Fig. 1).

Observed LPC content ranged from 0.5 to 12.9 mg l^{-1} over both spawning seasons (Fig. 2C, Table S1 in the Supplement at www.int-res.com/articles/suppl/m745p073_supp.pdf). Site-averaged LPC content in 2021 was greatest in early June but displayed 2 additional peaks in mid-August and late October. Only one major LPC peak occurred in 2022, from late-July to early-August. The effects of year, temperature, and the interaction between year and salinity were significant for LPC content, although salinity was not a significant main effect (Table 3). Average LPC content was greater (3.52 ± 2.43 mg l^{-1}) in 2021 than in 2022 (2.39 ± 1.68 mg l^{-1}). The P:LC ratio differed significantly across years, with the median ratio in 2021 (0.32) being lower than in 2022 (0.68; Fig. 2D). Lipid contributed a high fraction of LPC in 2021, whereas protein was typically the dominant biochemical constituent in 2022, as exhibited by the P:LC ratio (Fig. 2D).

The effect of year was significant on all individual biochemical constituents (Table 3). During the 2021 spawning season, lipid and carbohydrate contents were generally higher, and protein content was generally lower than in 2022. The effect of salinity was

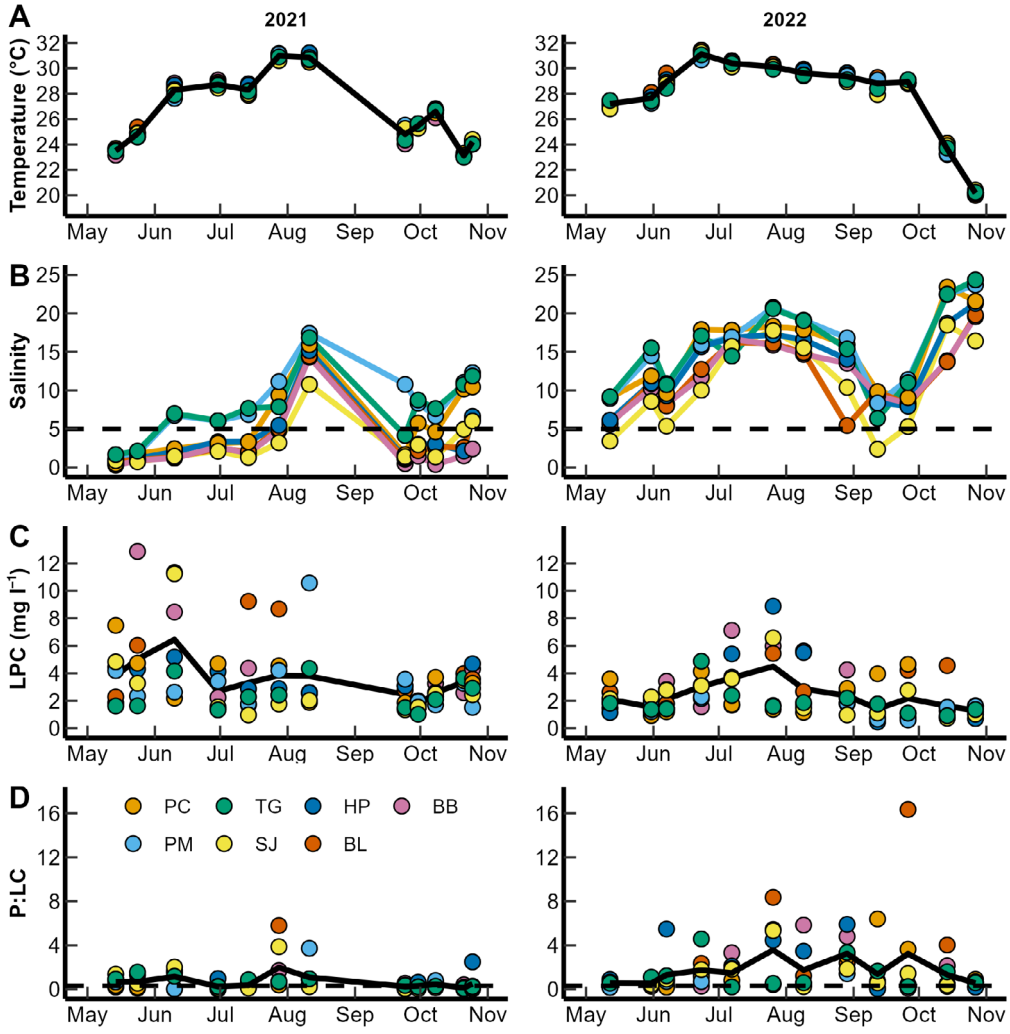

Fig. 2. Observed environmental and food conditions for the 2021 and 2022 reproductive seasons at each site (see Fig. 1 for site abbreviations). (A) Temperature, with the average measure presented by solid black lines; (B) salinity, with the oyster larval lower salinity growth threshold (5 ppt) indicated by the horizontal dashed lines for reference; (C) lipid, protein, and carbohydrate (LPC) content, with the average sound-wide value shown by the solid black lines; (D) protein-to-(lipid+carbohydrate) ratio, with the average P:LC ratio shown by the solid black lines and the median 2021 P:LC ratio (0.32) indicated by the horizontal dashed lines for comparison

only significant for carbohydrate content, but the interaction effect between year and salinity was significant for carbohydrate and protein contents. Temperature imposed a significant effect on both lipid and protein contents and the P:LC ratio but not on carbohydrate content. The interaction effect of year and temperature was only significant on lipid content (Table 3).

3.2. Model-estimated larval performance

3.2.1. Larval survivorship

The larval performance model estimated which phenotypes were capable of successful metamorphosis under observed environmental and food conditions at each site (Fig. 1) throughout the 2021 (Fig. 3) and 2022 (Fig. 4) spawning seasons. In 2021, estimated survivorship (successful metamorphosis; Fig. 3) was greatest at Telegraph (29.0%), followed by Pass Marianne (18.1%), Between Bridges (15.2%), and Henderson Point (13.8%). Survivorship was not predicted at Pass Christian, St. Joe, or Bay St. Louis. The period conducive to successful metamorphosis lasted from late June to mid-August, peaking in August, concurrent with the period of high salinity (Fig. 2B). A binomial test indicated that the proportion of viable simulation cases yielding surviving phenotypes across all sites in 2021 (0.157) was significantly different from what was expected, based on the proportion of viable cases in 2022 (0.657, $p < 0.0001$).

Table 1. Type III 2-way ANOVA summary table for the effects of observation year and site on temperature and salinity. Interaction terms were not significant ($p > 0.05$) and were removed from final ANOVA models

Effect	SS	df	*F*	p
Temperature				
Year	77.08	1	9.18	0.003
Site	1.65	6	0.03	0.999
Salinity				
Year	3085.73	1	151.78	<0.0001
Site	633.75	6	5.20	<0.0001

Table 2. Significant ($p \leq 0.05$) least-squares means results for pairwise comparison of salinity between sites (see Fig. 1). Non-significant pairwise comparisons ($p > 0.05$) were not tabulated

Contrast	Estimate	SE	df	*t*	p
BB–PM	−4.59	1.3	160	−3.52	0.010
BB–TG	−4.11	1.3	160	−3.16	0.031
BL–PM	−4.54	1.3	160	−3.42	0.014
BL–TG	−3.98	1.3	160	−3.06	0.041
SJ–PM	−5.15	1.3	160	−3.96	0.002
SJ–TG	−4.68	1.3	160	−3.60	0.008

All sites generated successfully metamorphosing larvae throughout the 2022 spawning season (Fig. 4). By site (Fig. 1), the greatest survivorship was estimated for Pass Marianne (68.0%), followed by Pass Christian (56.5%), Telegraph (41.4%), Bay St. Louis (32.1%), Between Bridges (26.0%), St. Joe (22.2%), and Henderson Point (18.4%). Peaks in metamorphic success occurred in early June, early August, and late September 2022, although site-specific trends varied (Fig. 4). Only 3 simulation cases generated 100% survivorship, all occurring in 2022; the average temperature, salinity, LPC content, and food quality parameters of these 40 d simulation periods are presented in Table 4.

The estimated proportion of successfully metamorphosing larvae across all sites during both years increased with increasing initial egg size and egg lipid content, as determined by the lipid multiplier (Fig. 5). Higher assimilation efficiency enhanced the likelihood of survivorship for each initial egg size and egg lipid content combination (Fig. 5). Survivorship at all assimilation efficiencies was lowest for phenotypes with initial egg sizes of <52 µm and lower egg lipid content (lipid multiplier of <0.8). Phenotypes were most successful with high assimilation efficiencies and egg sizes of ⩾60 µm, but higher initial egg lipid content ameliorated survival of smaller initial egg sizes.

Across both years, the central 80th percentile of PLDs from successful larvae varied between 16 and 36 d (median: 28 d). The central 80th percentile length at metamorphosis ranged between 313 and 380 µm (median: 346 µm). The effects of year and site were significant for both length at metamorphosis and PLD (Table 5). Successful phenotypes from 2021 were generally larger at metamorphosis (median: 350 µm) and took longer to develop (median: 31 d) than their 2022 counterparts (median length: 344 µm; median development time: 26 d). Within each year, the effect of site was also significant on final length and PLD (Table 6) as a result of spatiotemporal variation in exogenous conditions.

Table 3. Type III ANCOVA summary table for the main effects of year, salinity, and temperature on total food content (lipid, protein, carbohydrate; LPC) and the P:LC ratio. Only significant ($p \leq 0.05$) pairwise interaction effects were included in final models

Effect	SS	df	*F*	p
LPC				
Year	53.78	1	13.12	0.0004
Salinity	13.96	1	3.41	0.067
Temperature	50.13	1	12.23	0.0006
Year × salinity	21.59	1	5.27	0.023
Lipid				
Year	8.03	1	8.21	0.005
Salinity	0.01	1	0.01	0.926
Temperature	5.81	1	5.94	0.016
Year × temperature	4.90	1	5.10	0.027
Protein				
Year	12.32	1	5.22	0.024
Salinity	2.96	1	1.26	0.264
Temperature	56.87	1	24.10	<0.0001
Year × salinity	11.23	1	4.76	0.031
Carbohydrate				
Year	0.62	1	9.21	0.061
Salinity	1.74	1	25.86	<0.0001
Temperature	0.22	1	3.23	0.074
Year × salinity	1.04	1	15.46	0.0001
P:LC				
Year	16.92	1	5.31	0.022
Salinity	0.00	1	0.0001	0.992
Temperature	30.83	1	9.67	0.002

3.2.2. Larval mortality

The model reports several different potential sources of larval mortality resulting from the actions of various combinations of exogenous conditions on larval physiology. Most unsuccessful phenotypes simulated from the 2021 and 2022 environmental conditions and food supplies succumbed early to 'bad ini-

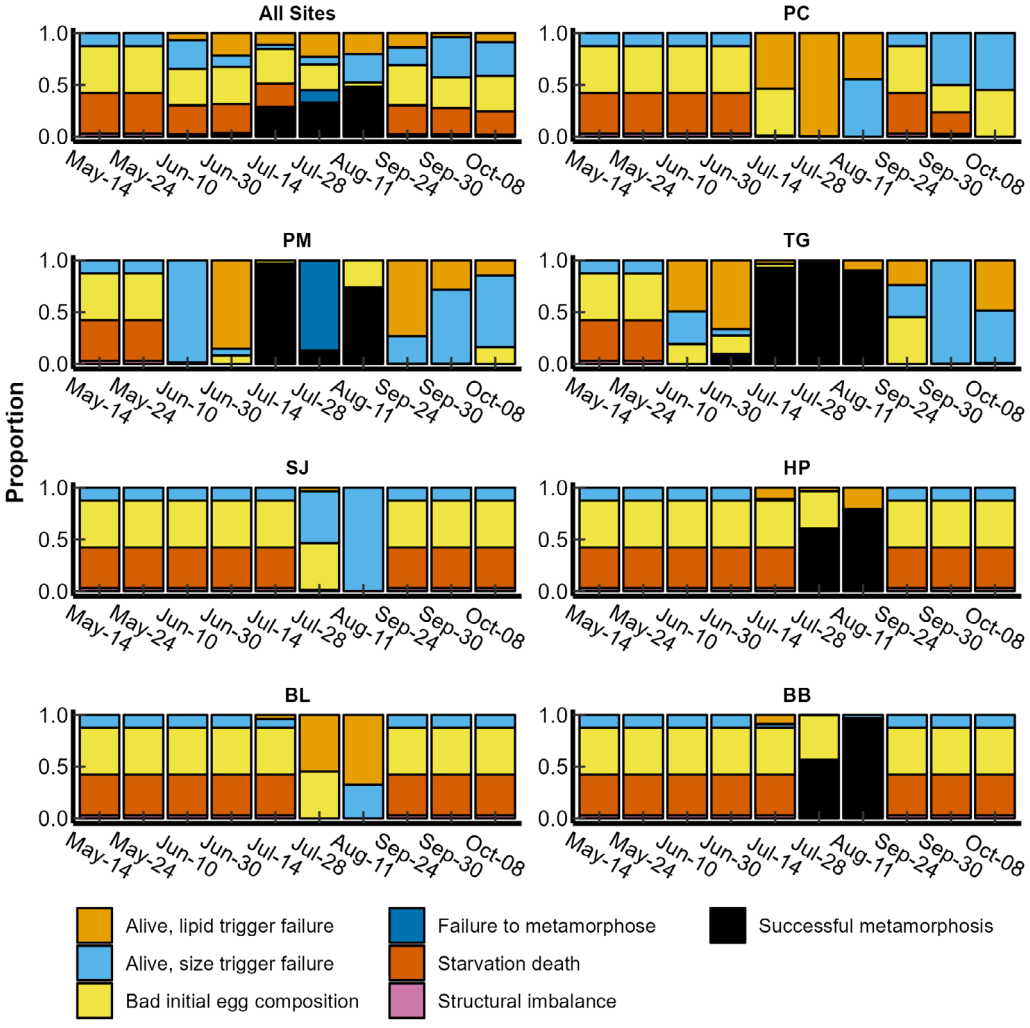

Fig. 3. Modeled larval performance for combined and individual sites (see Fig. 1 for site abbreviations) for the 2021 reproductive season. Each bar contains all phenotypes simulated for the given egg hatch date. Proportional performance outcomes (colored bars) are described as follows. 'Alive, lipid trigger failure': presumed nonmetabolic mortality. Larvae satisfy size criteria for attempted metamorphosis, but lipid imbalances prevent metamorphosis attempt before Day 40. 'Alive, size trigger failure': presumed nonmetabolic mortality. Larvae do not reach the 275 µm size threshold required for attempted metamorphosis. 'Bad initial egg composition': presumed mortality. Egg composition is inadequate for survival through Day 2. 'Failure to metamorphose': presumed mortality. Larvae satisfy criteria for attempted metamorphosis, but their neutral lipid stores, being less than their polar lipid stores, impedes successful metamorphosis. 'Starvation death': presumed mortality. The larval protein-to-ash ratio falls below the 0.7 minimal tolerable threshold. 'Structural imbalance': presumed mortality. Somatic polar lipid or carbohydrate stores become imbalanced in larvae and cannot be repaired by the other somatic stores or the neutral lipid stores. 'Successful metamorphosis': presumed survival. Larvae satisfy all criteria for attempted metamorphosis and contain sufficient neutral lipid stores to complete metamorphosis by Day 40

tial egg composition' (Figs. 3 & 4), the result of insufficient maternal lipid reserves to support early larval life stages. 'Starvation death' was pervasive in 2021 (Fig. 3) but less so in 2022 (Fig. 4), indicating that 2021 food supply inadequacies, particularly in protein content, hindered larval growth and development. In both years, many larvae remained alive at the end of the 40 d simulation period, failing to meet the size or lipid criteria necessary to attempt metamorphosis ('alive, lipid [or size] trigger failure'; Fig. 3). More larvae failed to reach a size conducing metamorphosis in 2021 (Fig. 3), while more failed in metamorphosis due to lipid storage deficiency in 2022 (Fig. 4). Mortality due to 'structural imbalance', mostly derived from an imbalance of protein and lipid supporting somatic growth, was a ubiquitous source of mortality in most 2021 simulations but accounted for a relatively minor proportion of overall mortality (Fig. 3). Biochemical imbalances were more prevalent in 2022, especially at Bay St. Louis (Fig. 4). 'Failure to metamorphose', when larvae satisfy the 25% neutral lipid reduction threshold but resultingly have insufficient energy

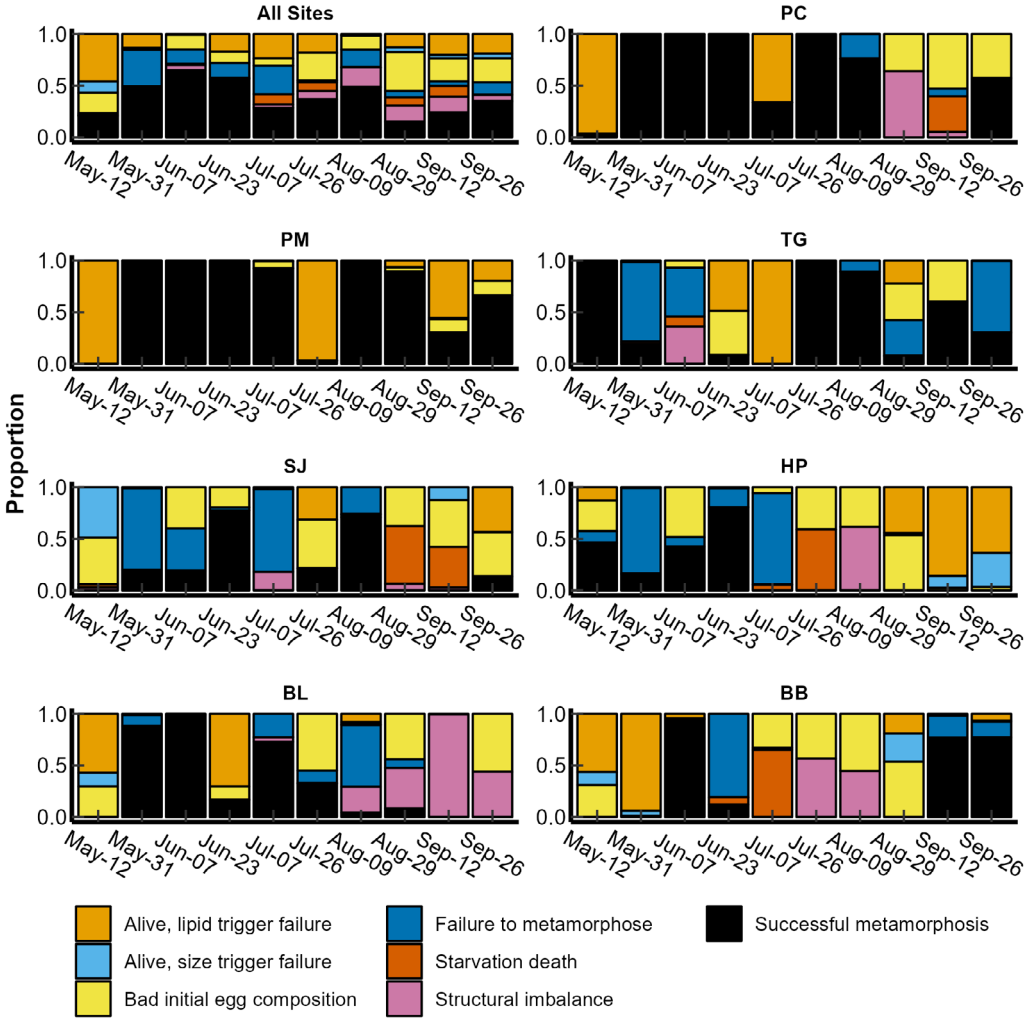

Fig. 4. Modeled larval performance for combined and individual sites (see Fig. 1 for site abbreviations) for the 2022 reproductive season. Each bar contains all phenotypes simulated for the given egg hatch date. Proportional performance outcomes (colored bars) are described in Fig. 3

stores to successfully metamorphose, was absent in 2021 except in late June at Pass Marianne (Fig. 3). By contrast, metamorphic failure was a common source of mortality at most sites in 2022 (Fig. 4).

Of the 140 simulations run across all sites and years, 82 yielded total mortality of all phenotypes. For 39 of the 82 total mortality cases, salinity remained <5 ppt for at least the first 11 simulation days; these cases generated identical larval performance outputs (i.e. 8 of 10 simulation cases from St. Joe in 2021; Fig. 3). In these low-salinity cases, the cause of mortality was specific to phenotypic combinations of initial egg size and lipid content but independent of assimilation efficiency. Cases of total mortality induced by low salinity originated from restricted larval feeding, as initial egg quality and the partitioning of biochemical com-

Table 4. Average 2022 temperature (T), salinity (S), total food content (lipid, protein, carbohydrate; LPC), and proportions of protein (P), polar lipid (PL), neutral lipid (NL), and carbohydrate (C) for simulation cases generating total phenotypic survival (see Fig. 1 for site abbreviations)

Site	Egg hatch date	T (°C)	S (ppt)	LPC (mg l^{-1})	P:LPC	PL:LPC	NL:LPC	C:LPC
PC	26 Jul 2022	29.6	17.2	1.94	0.51	0.13	0.13	0.23
TG	26 Jul 2022	29.4	17.8	1.97	0.54	0.15	0.15	0.16
PM	9 Aug 2022	29.3	14.5	1.40	0.45	0.13	0.13	0.29

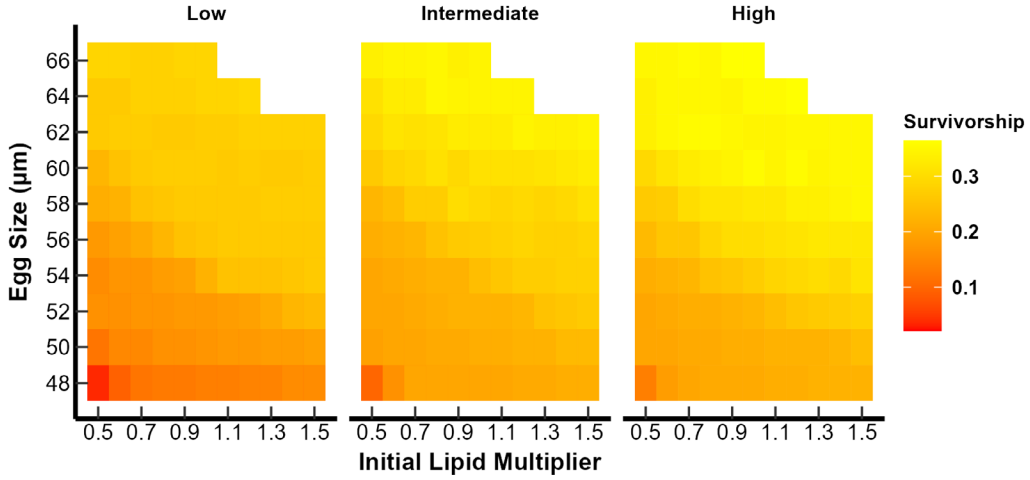

Fig. 5. Model-estimated survivorship of phenotypes across both reproductive seasons and all sites by initial egg size (n = 10) and lipid content multiplier (n = 11), for low (0.55, 0.6, 0.65), intermediate (0.7, 0.75, 0.8), and high (0.85, 0.9) assimilation efficiency (n = 8)

ponents post-fertilization proved insufficient to cover feeding limitations imposed by low salinity.

For the remaining 43 of 82 total mortality cases, salinity exceeded 5 ppt for most of the simulation period and did not completely restrict larval feeding. Complete mortality in these cases indicates severe food imbalances impeding phenotype survival. Mortality type was primarily governed by phenotypic variation interacting with inadequate food quantity or quality, although salinities between 5 and 10 ppt reduced feeding and growth rates (Figs. 3 & 4).

3.3. Settlement windows

3.3.1. Model-estimated settlement windows

Simulated larvae successfully metamorphosing in 2021 were restricted to settlement windows between 26 and 46 d (Fig. 6). The central 80th percentile of viable phenotypes settled between early August and mid-September, centered around late August. Model-estimated settlement windows were longer in 2022, between 34 and 146 d, as the central 80th percentile of viable phenotypes settled between late June and mid-October, centered around early August. Variations in settlement window durations existed across sites (Fig. 1) for both years (Fig. 6).

3.3.2. Observed settlement windows

Observed recruitment in 2022 was low across all sites, but highest at Pass Marianne and Telegraph (Fig. 7). At most surveyed sites (Fig. 1), peak recruitment occurred in July and August, gradually decreasing for the remainder of the spawning season. Peak recruitment at Pass Christian, however, occurred in September (Fig. 7). Estimated settlement calculated from recruitment observations occurred across all sites between May and September (Table 7). Site-specific settlement durations lasted between 46 and

Table 5. Type III 2-way ANOVA summary table for the main effects of year and site on modeled larval final length at metamorphosis and planktonic larval duration (PLD)

Effect	SS	df	*F*	p
Length				
Year	251286.9	1	438.91	<0.0001
Site	3980836.7	6	1158.85	<0.0001
PLD				
Year	76304.3	1	1568.19	<0.0001
Site	189873.3	6	650.37	<0.0001

Table 6. Type III ANOVA summary table for the effect of site on modeled larval final length at metamorphosis and planktonic larval duration (PLD) for the 2021 and 2022 reproductive seasons

Year	Effect	SS	df	*F*	p
2021	Length				
	Site	710680.1	3	708.96	<0.0001
	PLD				
	Site	236433.7	3	2809.97	<0.0001
2022	Length				
	Site	3916916.0	6	1068.19	<0.0001
	PLD				
	Site	898212.2	6	937.19	<0.0001

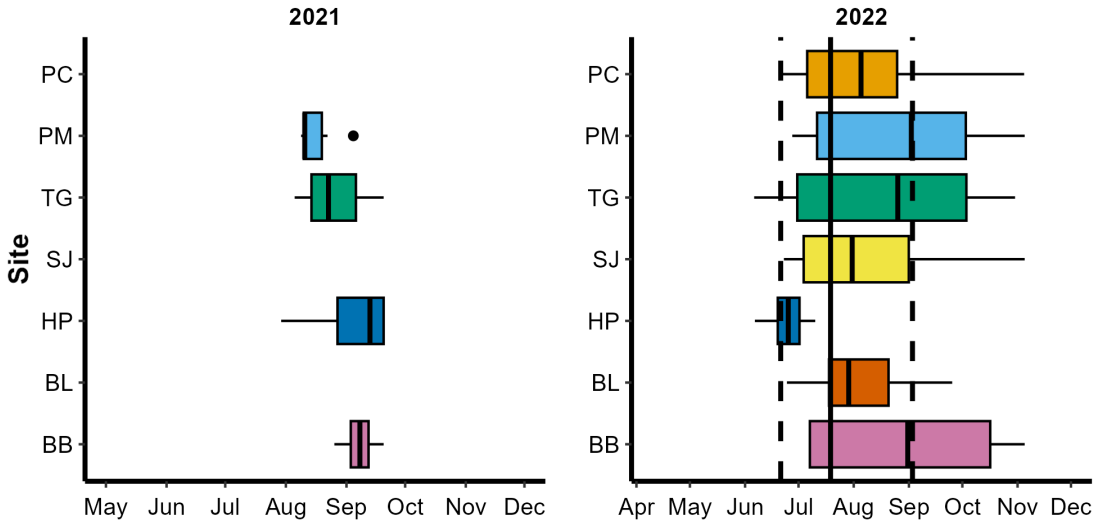

Fig. 6. Calculated settlement windows for the 2021 and 2022 reproductive seasons. Model-estimated settlement windows by site (see Fig. 1 for site abbreviations) are shown by the horizontal bars, with the median modeled settlement date indicated by the line within the interquartile range box. Whiskers present the complete modeled settlement window range, with outliers (values beyond 1.5 times the interquartile limits) shown by solid dots. The median 2022 sound-wide recruitment-derived settlement window is shown by the solid black vertical line, surrounded by the central 80th percentile settlement range represented by the dashed black vertical lines

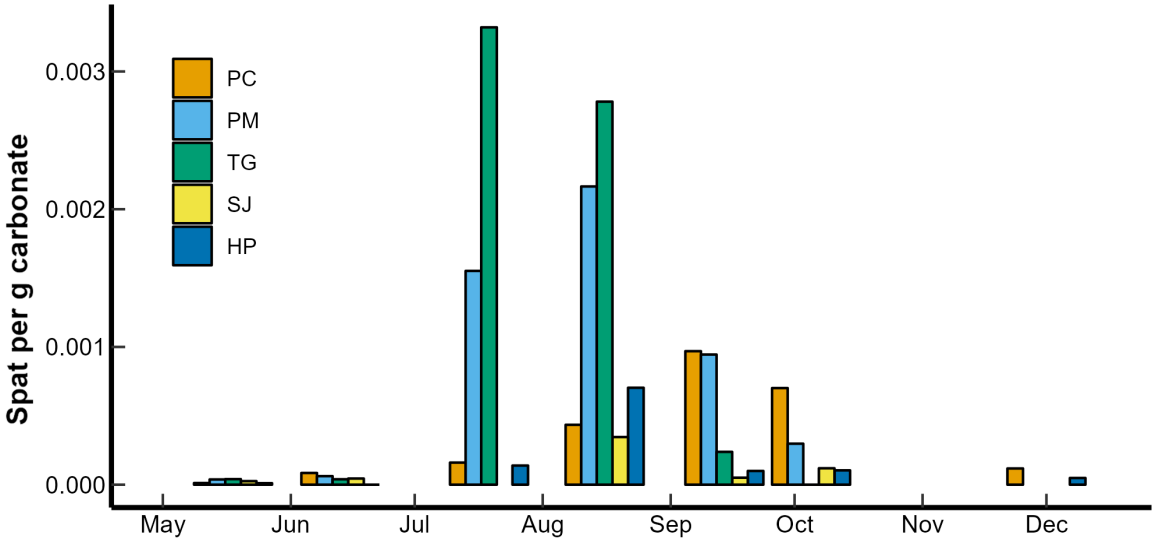

Fig. 7. Number of observed spat per gram carbonate by site (see Fig. 1 for site abbreviations) throughout the 2022 reproductive season. Missing bars indicate that surveying was not conducted for a particular site and time

111 d, spanning from late May to mid-September (Table 7). Across all surveyed sites (Fig. 1), the comprehensive settlement window occurred between late June and early September (Table 7, Fig. 6).

3.3.3. Comparing model-estimated and observed settlement windows

Model-estimated settlement windows for each site overlapped with observed recruitment-derived settlement windows, indicating strong agreement between model-estimated settlement and observed recruitment (Fig. 6). The larval model predicted settlement beyond what was observed at most sites (Fig. 1), but particularly at Pass Marianne, Telegraph, and Between Bridges (Fig. 6). Alignment between model-estimated settlement windows and the observed settlement window in 2022 was poorest for Henderson Point, although the median model-estimated settlement date still fell within the central 80th percentile range of the comprehensive observed settlement window (Fig. 6).

Table 7. The number of observed spat per site (see Fig. 1 for site abbreviations) in 2022 and subsequent calculated central 80th percentile settlement windows and durations. Surveys were not conducted at Bay St. Louis or Between Bridges

Site	n	10th percentile settlement date	Median settlement date	90th percentile settlement date	Settlement window duration (d)
PC	150	Jul 17	Aug 21	Sep 12	57
PM	287	Jun 20	Jul 19	Sep 3	75
TG	398	Jun 21	Jul 11	Aug 6	46
SJ	41	May 19	Jul 22	Sep 7	111
HP	47	Jun 21	Jul 29	Sep 10	81
Comprehensive	923	Jun 21	Jul 19	Sep 3	74

4. DISCUSSION

4.1. Model-estimated larval performance

4.1.1. Larval fate

The oyster (*Crassostrea virginica*) larval performance model identified periods when conditions were favorable for successful metamorphosis during the 2021 and 2022 spawning seasons in western Mississippi Sound. The model, however, cannot directly quantify survival and settlement of a true larval cohort in the field (Fig. 7). Rather, the model estimates the likelihood of survival given a suite of unweighted phenotypes subjected to exogenous conditions (Klein et al. 2023). The true scale of recruitment cannot be predicted because actual larval abundance and the distribution of phenotypic variation within larval cohorts are unknown. Nonetheless, the model does provide an estimate of survival and settlement potential given measures of temperature, salinity, food quantity, and food quality to which larvae in the field are exposed, in this case throughout the spawning seasons covering a 2 yr span in western Mississippi Sound.

Salinity, food supply, and phenotypic variation synergistically influence larval viability. The complex nature of collaborative endogenous (physiological variation) and exogenous (abiotic conditions) effects complicates identifying the principal causes of, or specific conditions for, larval success or failure. Regardless, simulation cases generating survival for the majority of phenotypes point to the importance of periods of favorable exogenous conditions, as the effects of suboptimal phenotypes were suppressed by advantageous temperature–salinity ranges and food supplies. Successful metamorphosis in 2021 was primarily governed by salinity, as larvae only survived concurrently with the late July to mid-August high-salinity regime. Under viable temperature–salinity conditions, however, food supply, as it interacts with phenotypic variation, controlled survivorship in model simulations. Favorable food supplies, paired with suitable environmental conditions, enabled a wider suite of phenotypes to survive (Bochenek et al. 2001, Powell et al. 2002, 2004, Hofmann et al. 2004, Klein et al. 2023).

Simulations from late July 2022 for Pass Christian and Telegraph and the early August 2022 simulation from Pass Marianne (Fig. 1) represent cases where favorable environmental conditions combined with near-optimal food supplies (Table 4) promoted 100% phenotype survival (Fig. 4). Similarly, cases of near-complete survivorship, such as during late May through early June 2022 at Pass Christian and Pass Marianne (Fig. 4), offered highly favorable conditions to promote successful metamorphosis amongst phenotypes, the only exceptions being those with 48 µm initial egg sizes, low initial egg lipid content, and generally low assimilation efficiencies. These phenotypes represent unfit physiological traits according to the model as indicated by poor larval performance across all cases (Fig. 5), as these larvae have minimal energy stores to meet metabolic demands and limited ability to accumulate energy from available food resources. Conversely, the model corroborates that phenotypes with high egg quality, determined in the model by egg size and egg lipid content (Fig. 5), are more fit for larval success (Gallager et al. 1986, Gallager & Mann 1986a,b). Assimilation efficiency is a secondary control (Fig. 5), as higher assimilation efficiencies allow for greater food intake and faster growth (Romberger & Epifanio 1981).

Periods of suboptimal exogenous conditions amplified the consequences of less fit phenotypes, restricting survivorship to only the fittest phenotypes (Klein et al. 2023). In extreme cases characterized by total mortality, the deleterious effects of unfavorable exogenous conditions were so severe that no phenotypic variant was able to counteract the external stressors. Time periods eliciting total mortality occurred in both years, albeit more frequent in 2021 (Fig. 3). These cases were either distinguished by prolonged extreme low salinity (<5 ppt), severe food imbalances, or a combination of unfavorable salinity (<7.5 ppt) and poor food supply. During 2021 and 2022, temperature remained within a favorable range (Dekshenieks et al. 1993) and did not contribute to mortality.

Total mortality consequent of low salinity was pervasive in 2021, but in 2022, only the late August St. Joe simulation generated low salinity-induced total mortality (Fig. 4). Telegraph and Pass Marianne, being closer to the open Gulf saltwater source (Fig. 1) (Eleuterius 1976), experienced higher salinity (Table 2), minimizing the occurrences of salinity-induced total mortality, while locations closer to freshwater inflows exhibited higher occurrences. Prolonged extreme low salinity, present from post-fertilization onward, always produced identical performance outcomes, specific to failure to survive upon first feeding once egg lipid stores are exhausted. Assimilation efficiency did not influence mortality, as metabolic processes controlling larval growth, including feeding, are limited under prolonged depressed salinity (Davis 1958, Dekshenieks et al. 1993, Lavaud et al. 2017, McFarland et al. 2022).

For total mortality cases in which salinity exceeded 5 ppt for most of the simulation period but remained below 10 ppt, food and salinity both contributed to poor larval performance. Larval feeding and growth occurred but at reduced rates compared to higher salinities (Dekshenieks et al. 1993). Low salinities heighten osmotic stress and metabolic processes (Davis 1958, Galtsoff 1964, Lavaud et al. 2017, Casas et al. 2018, McCarty et al. 2020) and lead to more rapid expenditure of maternal energy stores. For larvae to survive through metamorphosis under tolerable but stressful salinities, near-optimal food supply and favorable phenotypic configurations are required to offset the metabolic constraints imposed by lower salinity.

Some cases of total mortality occurred even when salinity was >12.5 ppt for the entire simulation period, such as both July 2022 simulations from Henderson Point and Between Bridges (Fig. 4). The effect of salinity on larval development is practically absent above 12.5 ppt (Dekshenieks et al. 1993, McFarland et al. 2022), indicating that food imbalances alone prevented survivorship. Along with favorable temperature–salinity conditions during these cases (Fig. 2), LPC content remained >3 mg l^{-1} for most of the simulation periods, suggesting food quantity did not impede performance either (Dekshenieks et al. 1993). Food quality was the dominant factor limiting survivorship, as protein was available in excess for these cases, while lipids were nearly absent (Fig. 2D).

A minimal threshold for food content surely exists (Dekshenieks et al. 1993, Bochenek et al. 2001), but the current model output suggests that food quality is more critical than food quantity. For instance, the model predicted high survivorship from late May through early June 2022 at Pass Marianne and Pass Christian (Fig. 4), despite LPC content remaining <2 mg l^{-1} (Fig. 2C) for most of the simulated durations, below the hypothesized optimal 3 mg l^{-1} threshold (Dekshenieks et al. 1993, Bochenek et al. 2001). Conversely, LPC content surpassed 4 mg l^{-1} in late July and early August 2022 at Henderson Point (Fig. 2C) but no larvae survived (Fig. 4). In both instances, salinity and temperature met tolerable thresholds (Fig. 2). In the latter cases, however, either protein or lipids were present in excess, while the other constituent was scarce (Fig. 2). High-protein diets are not conducive to larval development and success (Utting 1986, Bochenek et al. 2001), but neither are protein-depauperate diets (Klein et al. 2023). Although larval metabolism is lipid-based (Bochenek et al. 2001), some protein content threshold exists to maximize larval performance (Klein et al. 2023). Specific optimal food content and biochemical constituent proportions are difficult to identify, as dynamic environmental conditions and phenotypic composition in larvae influence feeding and energy expenditure differentially throughout larval development (Klein et al. 2023). Cases characterized by total survivorship, however, offer insight into highly favorable conditions given certain temperature–salinity ranges and phenotype distributions (Table 4).

4.1.2. Larval development

Larvae become competent to attempt metamorphosis at lengths of ⩾275 µm, but will continue to grow until minimal energy storage requisites are satisfied (Bochenek et al. 2001, Klein et al. 2023). Therefore, final larval lengths and PLDs are determined by the ability of larvae to accumulate sufficient energy stores (Klein et al. 2023). Simulated PLDs in both spawning seasons (median: 28 d) were consistent with observed *C. virginica* PLDs of approximately 20–30 d, though lifespan estimates as short as 15 d have been recorded (Ingle 1951, Carriker 1986, Kennedy 1996, Talmage & Gobler 2009). Additionally, the central 80th percentile of viable larval lengths at metamorphosis (313–378 µm) aligned with previous model estimations (Klein et al. 2023) and field findings (Nelson 1917, Carriker 1951, Loosanoff & Nomejko 1951, Nelson 1955, Loosanoff & Davis 1963, Kusaki 1991, Laing 1995). Successful larvae from 2021 simulations exhibited greater PLDs and lengths at metamorphosis than their 2022 counterparts (Table 5).

Food supply and phenotypic variation primarily controlled larval lifespan and final length. Relatively

higher lipid and lower protein content in 2021 (Table 3, Figs. 3 & 4) slowed larval growth and thus extended the time to reach metamorphic competency but promoted excessive neutral lipid stores. The overabundance of neutral lipids prevented the required 25% reduction within a single day, despite the amplified depletion of energy reserves once larvae reached lengths of ⩾250 µm (Bochenek et al. 2001). Thus, larvae continued to grow beyond the 275 µm size, albeit at a reduced rate, to a size large enough to trigger the proper neutral lipid reduction requisite for attempted metamorphosis. The recruitment trigger in the model is based on observed variations in lipid content at metamorphosis (Bochenek et al. 2001) but is to some extent hypothetical, as details of the physiological conditions triggering metamorphosis are poorly known (Collet et al. 1999, García-Esquivel et a. 2001, Rico-Villa et al. 2009). Furthermore, the model does not consider other influences such as settlement cues (Hidu et al. 1978, Fitt & Coon, 1992, Lillis et al. 2014, Pace et al. 2023). Recognizing this constraint, despite higher LPC content in 2021 than in 2022 (Table 3), time to metamorphosis was shorter in 2022, emphasizing the importance of food quality in determining larval performance (Klein et al. 2023). Although less abundant, available food in 2022 was more balanced to meet larval nutritional demands, as exhibited by median annual P:LC ratios (Fig. 2D) and comparable to favorable P:LC ratios reported in Klein et al. (2023) for Delaware Bay. The more balanced diets promoted rapid growth to metamorphosis compared to PLDs in 2021. Shorter larval durations enhance recruitment potential, as the risk of predation and transport away from suitable substrates are minimized (Cake 1983, Eckman 1996, Dekshenieks et al. 1997, Harding 1999, North et al. 2008, Knights et al. 2012).

4.2. Comparing settlement windows

Validating model-estimated settlement windows relied on knowledge of local spat growth to appropriately estimate settlement windows derived from recruitment observations (Klein et al. 2023). Pass Marianne, Telegraph, and St. Joe (Fig. 1) were not sampled in December 2022, which likely truncated the observed settlement window. Considering that spat were recorded at Henderson Point and Pass Christian during December surveys (Fig. 7), spat were likely present at the unsampled sites as well. Furthermore, December sampling was conducted 57 d after October sampling, which offered ample time for new recruits to settle and grow beyond the 25 mm spat length threshold. Thus, some late-season recruitment may have gone undetected, and the comprehensive observed settlement window is likely skewed toward earlier in the spawning season, which could explain why model-estimated settlement windows extend beyond the observed settlement window. Another potential explanation for prolonged model-estimated settlement beyond observed settlement windows may be a mismatch in exogenous conditions, namely food supply, and reproductive output in the field. That is, although the model predicted a period conducive to larval success, the timing of actual spawning events relative to viable exogenous conditions may not have aligned to yield late-season recruitment (Cushing 1990, Philippart et al. 2014).

Conversely, periods in which settlement was calculated from observed recruitment but not estimated by the model were likely due to model uncertainties, such as larval sensitivity to food imbalances (Bochenek et al. 2001, Klein et al. 2023). The model does not permit differential assimilation efficiencies specific to biochemical constituents and their relative proportion in available food. Therefore, during periods of excessive lipid or protein, simulated larvae cannot regulate their intake of one component to appropriately balance the remaining food supply. Additionally, protein interconversion with other components within the model is limited, which can impede proper balance between somatic components and energy stores (Bochenek et al. 2001).

Despite uncertainties in recruitment observations, spat growth rates in Mississippi Sound, and the larval model, model-estimated settlement windows from 2022 displayed good alignment to the concomitant settlement window derived from recruitment observations (Table 7, Fig. 6). Moreover, current estimated spawning and settlement patterns derived by both model efforts and recruitment observations were verified by local and regional records. Modeled egg hatch dates were viable for larval survivorship from May through September 2022 (Fig. 4), which is consistent with observed recruitment (Fig. 7) and aligns with documented northern Gulf of Mexico spawning seasons between May and October (Schlesselman 1955, Demoran 1966, Cake 1983). Observed recruitment climaxed between July and August 2022 at most sites (Fig. 7), which is consistent with Ogle (1979) but later than records from neighboring systems (Hopkins 1954, Hopkins et al. 1954, Hayes & Menzel 1981), although still within the overarching settlement range (Chatry et al. 1983).

A primary late spring peak in spawning followed by a secondary late summer pulse historically character-

ized northern Gulf of Mexico spawning dynamics (MacKenzie 1977, Cake 1983), as prolonged and sufficient environmental conditions and food supply permitted oysters to replenish their reproductive stores (Hofmann et al. 1994). Model output from 2022 illustrates this concept, as multiple peaks in spawning (egg hatch dates) were exhibited (Fig. 4). Observed recruitment, however, only portrayed a single peak between July and August (Fig. 7), which is consistent with spawning seasons estimated by Pace et al. (2020b), given anticipated larval lifespans between 20 and 30 d (Kennedy 1996), and suggests a shift in exogenous conditions limiting oysters from multiple spawns in a season in Mississippi Sound. One possible explanation is a reduction in food supply relative to historical conditions (e.g. Powell et al. 1995). Pace et al. (2020b) noted that gonadal and condition indices of mature oysters dropped substantially following spawns, which is to be expected. Unlike most Gulf of Mexico oyster populations (Soniat & Ray 1985), however, these health indices remained low afterward (Pace et al. 2020b). Failure of the condition index to rebound following the first spawn suggests a deficiency in food quantity or quality later in what would generally be considered the spawning season in most Gulf of Mexico oyster populations.

5. CONCLUSIONS

Strong agreement between model-estimated and observed settlement windows verifies the ability of the model to accurately identify periods of exogenous conditions conducive to larval survivorship. Field validation demonstrates that the model satisfactorily identifies how food supply and other environmental constraints contribute to local recruitment limitations. Notably, the model provides critical insight into the influence of food supply, and particularly food quality, on larval performance and settlement potential. The model has now been validated for *Crassostrea virginica* in Mississippi Sound and previously Delaware Bay (Klein et al. 2023), illustrating its broad applicability in various systems. Multiple successful validation efforts indicate that the model can be a tool to identify periods conducive for larval development and periods of unfavorable ambient conditions that restrict larval survival, both of which ultimately influence population maintenance, provided that appropriate food supply metrics are included in environmental monitoring programs.

Simulations support the conclusion that salinity and food supply primarily control larval performance and ultimately settlement potential in the recruitment-limited oyster populations of western Mississippi Sound. During periods of high reproductive output and favorable environmental conditions (i.e. salinity), food supply predominantly governs larval performance and settlement potential. A sufficiently balanced food supply will promote larval survival and thus population growth and recovery, but an inadequate food supply will contribute to recruitment limitations. Of particular importance is the P:LC ratio, identified in the model as a key contributor to larval performance or failure (Klein et al. 2023).

Moreover, the effects of food supply and salinity are often synergistic, both positively and negatively. Freshwater inflows disrupt salinity regimes and influence the amount and assemblage of phytoplankton and other organic materials available as food (Kreeger et al. 1997, Seitzinger et al. 2002, Carmichael et al. 2004, Roelke et al. 2013, Camacho et al. 2015, Riekenberg et al. 2015, Parra et al. 2020). Considering that freshwater intrusions frequently impact oyster population stability (Munroe et al. 2013, Parker et al. 2013, Soniat et al. 2013, Gledhill et al. 2020), examining larval responses to changing environmental conditions and food regimes during and after disturbance events may provide important insight into understanding the time history and success of population recovery (Dekshenieks et al. 2000, Powell et al. 2003).

Critical gaps persist in the understanding of oyster larval food supply and feeding, particularly in precise metrics related to the composition of the food assemblage, including particle size and biochemical quality (e.g. Baldwin & Newell 1991, 1995a,b). Subsequent studies should evaluate the influence of food particle size distribution and relative nutritional quality on larval assimilation rates to properly understand their impacts on oyster larval performance and recruitment dynamics.

Western Mississippi Sound remains susceptible to ongoing disruptions in larval recruitment caused by freshwater influxes, either by openings of the Bonnet Carré Spillway or periods of extreme precipitation. Given the current state of local oyster beds (Gledhill et al. 2020, Morgan & Rakocinski 2022) and potential shift in food supply, populations lack the resilience to withstand such highly adverse episodes and are susceptible to further mass mortality events and population collapses (Pace et al. 2020a,b, 2023, Pruett et al. 2024). Observations by Pace et al. (2020b) and results herein suggest that the current realized spawning season has been curtailed (i.e. shortened) relative to earlier times, with the possibility that the underlying process is a modification in available food for both

adults and larvae. Truncated spawning seasons would exacerbate impediments to population recovery, as a shorter spawning season would likely yield a smaller overall larval cohort. Given food inadequacies experienced both by broodstock and larvae, eggs would likely be less fit (Gallager & Mann 1986a, Powell et al. 2011) and larvae would be exposed to more strenuous external conditions. These compounding challenges, if present, would be difficult to overcome, restricting oyster population resiliency. A further examination into this possibility seems worthwhile.

Acknowledgements. The present work was part of J.C.K.'s MSc thesis. The authors thank T. P. Wissing for field sampling assistance. This project was partially funded by the US Department of the Treasury, the Mississippi Department of Environmental Quality, and the Mississippi Based RESTORE Act Center of Excellence under the Resources and Ecosystems Sustainability, Tourist Opportunities, and Revived Economies of the Gulf Coast States Act of 2012 (RESTORE Act). The statements, findings, conclusions, and recommendations are those of the authors and do not necessarily reflect the views of the Department of the Treasury, the Mississippi Department of Environmental Quality, or the Mississippi Based RESTORE Act Center of Excellence. The authors also acknowledge support by a Non-Academic Research Internship for Graduate Students from the National Science Foundation (NSF) to J.C.K. under NSF award no. 1841112.

LITERATURE CITED

Andrews JD, Haven D, Quayle DB (1959) Fresh-water kill of oysters (*Crassostrea virginica*) in James River, Virginia, 1958. Proc Natl Shellfish Assoc 49:29–49

Baldwin BS, Newell RIE (1991) Omnivorous feeding by planktotrophic larvae of the eastern oyster *Crassostrea virginica.* Mar Ecol Prog Ser 78:285–301

Baldwin BS, Newell RIE (1995a) Feeding rate responses of oyster larvae (*Crassostrea virginica*) to seston quantity and composition. J Exp Mar Biol Ecol 189:77–91

Baldwin BS, Newell RIE (1995b) Relative importance of different size food particles in the natural diet of oyster larvae (*Crassostrea virginica*). Mar Ecol Prog Ser 120:135–145

Barnes BB, Luckenbach MW, Kingsley-Smith PR (2010) Oyster reef community interactions: the effect of resident fauna on oyster (*Crassostrea* spp.) larval recruitment. J Exp Mar Biol Ecol 391:169–177

Beck MW, Brumbaugh RD, Airoldi L, Carranza A and others (2011) Oyster reefs at risk and recommendations for conservation, restoration, and management. Bioscience 61: 107–116

Ben Kheder R, Moal J, Robert R (2010) Impact of temperature on larval development and evolution of physiological indices in *Crassostrea gigas.* Aquaculture 309:286–289

Berg JA, Newell RIE (1986) Temporal and spatial variations in the composition of seston available to the suspension feeder *Crassostrea virginica.* Estuar Coast Shelf Sci 23: 375–386

Bochenek EA, Klinck JM, Powell EN, Hofmann EE (2001) A biochemically based model of the growth and development of *Crassostrea gigas* larvae. J Shellfish Res 20: 243–265

Brammer AJ, Rodriguez Del Rey Z, Spalding EA, Poirrier MA (2007) Effects of the 1997 Bonnet Carré Spillway opening on infaunal macroinvertebrates in Lake Pontchartrain, Louisiana. J Coast Res 23:1292–1303

Brumbaugh RD, Coen LD (2009) Contemporary approaches for small-scale oyster reef restoration to address substrate versus recruitment limitation: a review and comments relevant for the Olympia oyster, *Ostrea lurida* Carpenter 1864. J Shellfish Res 28:147–161

Brunner EL, Prahl FG, Hales B, Waldbusser GG (2016) A longitudinal study of Pacific oyster (*Crassostrea gigas*) larval development: isotope shifts during early shell formation reveal sub-lethal energetic stress. Mar Ecol Prog Ser 555:109–123

Butler PA (1952) Effect of floodwaters on oysters in Mississippi Sound in 1950. US Fish Wildl Serv Res Rep 31:1–20

Butler PA (1953) Oyster growth as affected by latitudinal temperature gradients. Comm Fish Rev 15:7–12

Cake EW (1983) Habitat suitability index models: Gulf of Mexico American oyster. FWS/OBS-82/10/57. US Department of the Interior, Fish and Wildlife Service, Washington, DC

Camacho RA, Martin JL, Watson B, Paul MJ, Zheng L, Stribling JB (2015) Modeling the factors controlling phytoplankton in the St. Louis Bay Estuary, Mississippi and evaluating estuarine responses to nutrient load modifications. J Environ Eng 141:04014067

Carmichael RH, Shriver AC, Valiela I (2004) Changes in shell and soft tissue growth, tissue composition, and survival of quahogs, *Mercenaria mercenaria*, and softshell clams, *Mya arenaria*, in response to eutrophic-driven changes in food supply and habitat. J Exp Mar Biol Ecol 313:75–104

Carriker MR (1951) Ecological observations on the distribution of oyster larvae in New Jersey estuaries. Ecol Monogr 21:19–38

Carriker MR (1986) Influence of suspended particles on biology of oyster larvae in estuaries. Am Malacol Bull Spec Edn 3:41–49

Casas SM, Lavaud R, La Peyre MK, Comeau LA, Filgueira R, La Peyre JF (2018) Quantifying salinity and season effects on eastern oyster clearance and oxygen consumption rates. Mar Biol 165:90

Chatry M, Dugas RJ, Easley KA (1983) Optimum salinity regime for oyster production on Louisiana's state seed grounds. Contrib Mar Sci 26:81–94

Coen LD, Luckenbach MW (2000) Developing success criteria and goals for evaluating oyster reef restoration: Ecological function or resource exploitation? Ecol Eng 15: 323–343

Coen LD, Brumbaugh RD, Bushek D, Grizzle R and others (2007) Ecosystem services related to oyster restoration. Mar Ecol Prog Ser 341:303–307

Collet B, Boudry P, Thebault A, Heurtebise S, Morand B, Gérard A (1999) Relationship between pre- and post-metamorphic growth in the Pacific oyster *Crassostrea gigas* (Thunberg). Aquaculture 175:215–226

Cushing DH (1990) Plankton production and year-class strength in fish populations: an update of the match/mismatch hypothesis. Adv Mar Biol 26:249–293

Da Costa F, Petton B, Mingant C, Bougaran G and others (2016) Influence of one selected *Tisochrysis lutea* strain rich in lipids on *Crassostrea gigas* larval development and biochemical composition. Aquacult Nutr 22:813–836

Davis HC (1958) Survival and growth of clam and oyster larvae at different salinities. Biol Bull (Woods Hole) 114: 296–307

Davis HC, Calabrese A (1964) Combined effects of temperature and salinity on the development of eggs and growth of larvae of *Mercenaria mercenaria* and *Crassostrea virginica.* Fish Bull 63:643–655

De Santiago K, Palmer TA, Dumesnil M, Pollack JB (2019) Rapid development of a restored oyster reef facilitates habitat provision for estuarine fauna. Restor Ecol 27: 870–880

Dekshenieks MM, Hofmann EE, Powell EN (1993) Environmental effects on the growth and development of eastern oyster, *Crassostrea virginica* (Gmelin, 1791), larvae: a modeling study. J Shellfish Res 12:241–254

Dekshenieks MM, Hofmann EE, Klinck JM, Powell EN (1997) A modeling study of the effects of size- and depth-dependent predation on larval survival. J Plankton Res 19:1583–1598

Dekshenieks MM, Hofmann EE, Klinck JM, Powell EN (2000) Quantifying the effects of environmental change on an oyster population: a modeling study. Estuaries 23: 593–610

Demoran WJ (1966) Homes for oysters. Miss Game Fish 26: 12–13

Du J, Park K, Jensen C, Dellapenna TM, Zhang WG, Shi Y (2021) Massive oyster kill in Galveston Bay caused by prolonged low-salinity exposure after Hurricane Harvey. Sci Total Environ 774:145132

Dunn RP, Eggleston DB, Lindquist N (2014) Effects of substrate type on demographic rates of eastern oyster (*Crassostrea virginica*). J Shellfish Res 33:177–185

Eckman JE (1996) Closing the larval loop: linking larval ecology to the population dynamics of marine benthic invertebrates. J Exp Mar Biol Ecol 200:207–237

Eierman LE, Hare MP (2013) Survival of oyster larvae in different salinities depends on source population within an estuary. J Exp Mar Biol Ecol 449:61–68

Eleuterius CK (1976) Mississippi Sound: salinity distribution and indicated flow patterns. Sea Grant Publication MASGP-76-023. Mississippi–Alabama Sea Grant Consortium, Ocean Springs, MS

Eleuterius CK (1977) Location of the Mississippi Sound oyster reefs as related to salinity of bottom waters during 1973–1975. Gulf Caribb Res 6:17–23

Eleuterius CK (1978) Classification of Mississippi Sound as to estuary hydrological type. Gulf Caribb Res 6:185–187

Fach BA, Hofmann EE, Murphy EJ (2002) Modeling studies of Antarctic krill *Euphausia superba* survival during transport across the Scotia Sea. Mar Ecol Prog Ser 231: 187–203

Fitt WK, Coon SL (1992) Evidence for ammonia as a natural cue for recruitment of oyster larvae to oyster beds in a Georgia salt marsh. Biol Bull (Woods Hole) 182:401–408

Flores-Vergara C, Cordero-Esquivel B, Ceron-Ortiz AN, Arredondo-Vega BO (2004) Combined effects of temperature and diet on growth and biochemical composition of the Pacific oyster *Crassostrea gigas* (Thunberg) spat. Aquacult Res 35:1131–1140

Fodrie FJ, Rodriguez AB, Gittman RK, Grabowski JH and others (2017) Oyster reefs as carbon sources and sinks. Proc R Soc B 284:20170891

Fox J, Weisberg S (2019) An R companion to applied regression, 3rd edn. Sage, Thousand Oaks, CA. https://socialsciences.mcmaster.ca/jfox/Books/Companion

Fulford RS, Breitburg DL, Luckenbach M, Newell RIE (2010) Evaluating ecosystem response to oyster restoration and nutrient load reduction with a multispecies bioenergetics model. Ecol Appl 20:915–934

Gallager SM, Mann R (1986a) Growth and survival of larvae of *Mercenaria mercenaria* (L.) and *Crassostrea virginica* (Gmelin) relative to broodstock conditioning and lipid content of eggs. Aquaculture 56:105–121

Gallager SM, Mann R (1986b) Individual variability in lipid content of bivalve larvae quantified histochemically by absorption photometry. J Plankton Res 8:927–937

Gallager SM, Mann R, Sasaki GC (1986) Lipid as an index of growth and viability in three species of bivalve larvae. Aquaculture 56:81–103

Galtsoff PS (1964) The American oyster *Crassostrea virginica* Gmelin. Fish Bull (Wash DC) 64:1–480

García-Esquivel Z, Bricelj VM, González-Gómez MA (2001) Physiological basis for energy demands and early post-larval mortality in the Pacific oyster, *Crassostrea gigas.* J Exp Mar Biol Ecol 263:77–103

Gledhill JH, Barnett AF, Slattery M, Willett KL, Easson GL, Otts SS, Gochfeld DJ (2020) Mass mortality of the eastern oyster *Crassostrea virginica* in the western Mississippi Sound following unprecedented Mississippi River flooding in 2019. J Shellfish Res 39:235–244

Grabowski JH, Brumbaugh RD, Conrad RF, Keeler AG and others (2012) Economic valuation of ecosystem services provided by oyster reefs. Bioscience 62:900–909

Grabowski JH, Powers SP, Roman H, Rouhani S (2017) Potential impacts of the 2010 *Deepwater Horizon* oil spill on subtidal oysters in the Gulf of Mexico. Mar Ecol Prog Ser 576:163–174

Gunter G (1953a) The Bonnet Carré Spillway and the oyster beds of Mississippi Sound. Conv Add Natl Shellfish Assoc 1951:46

Gunter G (1953b) The relationship of the Bonnet Carré Spillway to oyster beds in Mississippi Sound and the 'Louisiana Marsh,' with a report on the 1950 opening. Contrib Mar Sci 3:17–71

Hall AS, Méthé D, Stewart-Clark SE, Clark KF, Tremblay R (2020) Comparison of absorption efficiency and metabolic rate between wild and aquaculture oysters (*Crassostrea virginica*). Aquacult Rep 16:100263

Harding JM (1999) Selective feeding behavior of larval naked gobies *Gobiosoma bosc* and blennies *Chasmodes bosquianus* and *Hypsoblennius hentzi*: preferences for bivalve veligers. Mar Ecol Prog Ser 179:145–153

Harding JM, Mann R (2001) Oyster reefs as fish habitat: opportunistic use of restored reefs by transient fishes. J Shellfish Res 20:951–959

Hayes PF, Menzel RW (1981) The reproductive cycle of early setting *Crassostrea virginica* (Gmelin) in the northern Gulf of Mexico, and its implications for population recruitment. Biol Bull (Woods Hole) 160:80–88

Hemeon KM, Ashton-Alcox KA, Powell EN, Pace SM, Poussard LM, Solinger LK, Soniat TM (2020) Novel shell stock–recruitment models for *Crassostrea virginica* as a function of regional shell effective surface area, a missing link for sustainable management. J Shellfish Res 39:633–654

Hendriks IE, Van Duren LA, Herman PMJ (2003) Effect of dietary polyunsaturated fatty acids on reproductive output and larval growth of bivalves. J Exp Mar Biol Ecol 296:199–213

Hesterberg SG, Herbert GS, Pluckhahn TJ, Harke RM and others (2020) Prehistoric baseline reveals substantial

decline of oyster reef condition in a Gulf of Mexico conservation priority area. Biol Lett 16:20190865
Hidu H, Valleau WG, Veitch FP (1978) Gregarious setting in European and American oysters — response to surface chemistry vs. waterborne pheromones. Proc Natl Shellfish Assoc 68:11–16
His E, Seaman MNL (1992) Effects of temporary starvation on the survival, and on subsequent feeding and growth, of oyster (*Crassostrea gigas*) larvae. Mar Biol 114:277–279
Hofmann EE, Powell EN, Klinck JM, Wilson EA (1992) Modeling oyster populations III. Critical feeding periods, growth and reproduction. J Shellfish Res 11:399–416
Hofmann EE, Klinck JM, Powell EN, Boyles S, Ellis M (1994) Modeling oyster populations II. Adult size and reproductive effort. J Shellfish Res 13:165–182
Hofmann EE, Powell EN, Bochenek EA, Klinck JM (2004) A modelling study of the influence of environment and food supply on survival of *Crassostrea gigas* larvae. ICES J Mar Sci 61:596–616
Hopkins SH (1954) Oyster setting on the Gulf coast. Proc Natl Shellfish Assoc 45:52–55
Hopkins SH, Mackin JG, Menzel RW (1954) The annual cycle of reproduction, growth and fattening in Louisiana oysters. Proc Natl Shellfish Assoc 1953:39–50
Ingle RM (1951) Spawning and setting of oysters in relation to seasonal environmental changes. Bull Mar Sci 1: 111–135
Ingle RM, Dawson CE (1952) Growth of the American oyster, *Crassostrea virginica* (Gmelin) in Florida waters. Bull Mar Sci Gulf Caribb 2:393–403
Kennedy VS (1996) Biology of larvae and spat. In: Kennedy VS, Newell RIE, Eble AF (eds) The eastern oyster: *Crassostrea virginica*. Maryland Sea Grant, College Park, MD, p 371–411
Kennedy VS, Newell RIE, Krantz GE, Otto S (1995) Reproductive capacity of the eastern oyster *Crassostrea virginica* infected with the parasite *Perkinsus marinus.* Dis Aquat Org 23:135–144
Klein JC, Powell EN, Kreeger DA, Ashton-Alcox KA and others (2023) Modeling eastern oyster (*Crassostrea virginica*) larval performance and settlement windows in Delaware Bay. J Shellfish Res 42:437–463
Knights AM, Walters K (2010) Recruit–recruit interactions, density-dependent processes and population persistence in the eastern oyster *Crassostrea virginica.* Mar Ecol Prog Ser 404:79–90
Knights AM, Firth LB, Walters K (2012) Interactions between multiple recruitment drivers: post-settlement predation mortality and flow-mediated recruitment. PLOS ONE 7: e35096
Kraeuter JN, Castagna M, van Dessel R (1981) Egg size and larval survival of *Mercenaria mercenaria* (L.) and *Argopecten irradians* (Lamarck). J Exp Mar Biol Ecol 56:3–8
Kraeuter JN, Ford S, Cummings M (2007) Oyster growth analysis: a comparison of methods. J Shellfish Res 26: 479–491
Kreeger DA, Goulden CE, Kilham SS, Lynn SG, Datta S, Interlandi SJ (1997) Seasonal changes in the biochemistry of lake seston. Freshw Biol 38:539–554
Kusaki Y (1991) Oyster culture in Japan and adjacent countries: *Crassostrea gigas* (Thunberg). In: Menzel W (ed) Estuarine and marine bivalve mollusk culture. CRC Press, Boca Raton, FL, p 227–243
La Peyre MK, Eberline BS, Soniat TM, La Peyre JF (2013) Differences in extreme low salinity timing and duration differentially affect eastern oyster (*Crassostrea virginica*) size class growth and mortality in Breton Sound, LA. Estuar Coast Shelf Sci 135:146–157
La Peyre MK, Aguilar Marshall D, Miller LS, Humphries AT (2019) Oyster reefs in northern Gulf of Mexico estuaries harbor diverse fish and decapod crustacean assemblages: a meta-synthesis. Front Mar Sci 6:666
Laing I (1995) Effect of food supply on oyster spatfall. Aquaculture 131:315–324
Lane RR, Day JW, Kemp GP, Demcheck DK (2001) The 1994 experimental opening of the Bonnet Carré Spillway to divert Mississippi River water into Lake Pontchartrain, Louisiana. Ecol Eng 17:411–422
Langdon C, Evans F, Jacobson D, Blouin M (2003) Yields of cultured Pacific oysters *Crassostrea gigas* Thunberg improved after one generation of selection. Aquaculture 220:227–244
Lavaud R, La Peyre MK, Casas SM, Bacher C, La Peyre JF (2017) Integrating the effects of salinity on the physiology of the eastern oyster, *Crassostrea virginica*, in the northern Gulf of Mexico through a dynamic energy budget model. Ecol Modell 363:221–233
Lenth RV (2023) emmeans: estimated marginal means, aka least-squares means. R package version 1.8.7. https://CRAN.R-project.org/package=emmeans
Lillis A, Eggleston DB, Bohnenstiehl DR (2014) Soundscape variations from a larval perspective: the case for habitat-associated sound as a settlement cue for weakly swimming estuarine larvae. Mar Ecol Prog Ser 509:57–70
Lipcius RN, Burke RP, McCulloch DN, Schreiber SJ, Schulte DM, Seitz RD, Shen J (2015) Overcoming restoration paradigms: value of the historical record and metapopulation dynamics in native oyster restoration. Front Mar Sci 2:65
Livingston RJ, Howell RL, Niu X, Lewis FG, Woodsum GC (1999) Recovery of oyster reefs (*Crassostrea virginica*) in a Gulf estuary following disturbance by two hurricanes. Bull Mar Sci 64:465–483
Loosanoff VL, Davis HC (1963) Rearing of bivalve mollusks. Adv Mar Biol 1:1–136
Loosanoff VL, Nomejko CA (1951) Spawning and setting of the American oyster, *Ostrea virginica*, in relation to lunar phases. Ecology 32:113–134
MacKenzie CL (1977) Development of an aquacultural program for rehabilitation of damaged oyster reefs in Mississippi Sound. Mar Fish Rev 39:1–13
MacKenzie CL (2007) Causes underlying the historical decline in eastern oyster (*Crassostrea virginica* Gmelin, 1791) landings. J Shellfish Res 26:927–938
Mann R, Powell EN (2007) Why oyster restoration goals in the Chesapeake Bay are not and probably cannot be achieved. J Shellfish Res 26:905–917
Manuel EC, Hare MP, Munroe D (2023) Consequences of salinity change, salinity history, and shell morphology on early growth of juvenile oysters. J Shellfish Res 42:21–28
Matias D, Ben-Hamadou R, Joaquim S, Matias AM, Sobral P, Leitão A (2015) The influence of different microalgal diets on European clam (*Ruditapes decussatus*, Linnaeus, 1758) larvae culture performances. Aquacult Res 46: 2527–2543
McCarty AJ, McFarland K, Small J, Allen SK, Plough LV (2020) Heritability of acute low salinity survival in the eastern oyster (*Crassostrea virginica*). Aquaculture 529: 735649
McDonald P, Rateliffo S, Guo X (2023) Fitness of wild and

selected eastern oyster (*Crassostrea virginica*) larvae under different conditions. J Shellfish Res 42:15–30

McFarland K, Plough LV, Nguyen M, Hare MP (2020) Are bivalves susceptible to domestication selection? Using starvation tolerance to test for potential trait changes in eastern oyster larae. PLOS ONE 15:e0230222

McFarland K, Vignier J, Standen E, Volety AK (2022) Synergistic effects of salinity and temperature on the eastern oyster *Crassostrea virginica* throughout the lifespan. Mar Ecol Prog Ser 700:111–124

Moran AL, Manahan DT (2004) Physiological recovery from prolonged 'starvation' in larvae of the Pacific oyster *Crassostrea gigas.* J Exp Mar Biol Ecol 306:17–36

Morgan LM, Rakocinski CF (2022) Predominant factors limiting the recovery of the eastern oyster (*Crassostrea virginica*) in western Mississippi Sound, USA. Estuar Coast Shelf Sci 264:107652

Munroe D, Tabatabai A, Burt I, Bushek D, Powell EN, Wilkin J (2013) Oyster mortality in Delaware Bay: impacts and recovery from Hurricane Irene and Tropical Storm Lee. Estuar Coast Shelf Sci 135:209–219

Munroe D, Borsetti S, Ashton-Alcox K, Bushek D (2017) Early post-settlement growth in wild eastern oyster (*Crassostrea virginica* Gmelin 1791) populations. Estuaries Coasts 40:880–888

Nelson J (1917) An investigation of oyster propagation in Richmond Bay, PEI, during 1915. Contrib Can Biol Fish 1915–16:53–78

Nelson TC (1955) Observations of the behavior and distribution of oyster larvae. Proc Natl Shellfish Assoc 45: 23–28

North EW, Schlag Z, Hood RR, Li M, Zhong L, Gross T, Kennedy VS (2008) Vertical swimming behavior influences the dispersal of simulated oyster larvae in a coupled particle-tracking and hydrodynamic model of Chesapeake Bay. Mar Ecol Prog Ser 359:99–115

Ogle J (1979) A study of four oyster reefs in Mississippi. Gulf Res Rep 6:261–265

Osman RW, Whitlatch RB, Zajac RN (1989) Effects of resident species on recruitment into a community: larval settlement versus post-settlement mortality in the oyster *Crassostrea virginica*. Mar Ecol Prog Ser 54:61–73

Pace SM, Poussard LM, Powell EN, Ashton-Alcox KA and others (2020a) Dying, decaying, and dissolving into irrelevance: first direct in-the-field estimate of *Crassostrea virginica* shell loss—a case history from Mississippi Sound. J Shellfish Res 39:245–256

Pace SM, Powell EN, Soniat TM, Kuykendall KM (2020b) How oyster health indices vary between mass mortality events. J Shellfish Res 39:603–617

Pace SM, Powell EN, Kuykendall KM, Soniat TM (2023) Effective surface area and the potential for recovery from mass mortality in eastern oyster populations, with a vignette on the critical period for reef recovery. J Shellfish Res 42:241–254

Parker ML, Arnold WS, Geiger SP, Gorman P, Leone EH (2013) Impacts of freshwater management activities on eastern oyster (*Crassostrea virginica*) density and recruitment: recovery and long-term stability in seven Florida estuaries. J Shellfish Res 32:695–708

Parra SM, Sanial V, Boyette AD, Cambazoglu MK and others (2020) Bonnet Carré Spillway freshwater transport and corresponding biochemical properties in the Mississippi Bight. Cont Shelf Res 199:104114

Pfeiffer-Hoyt AS, McManus MA (2005) Modeling the effects of environmental variability on *Balanus glandula* larval development. J Plankton Res 27:1211–1228

Philippart CJM, Bleijswijk JDL, Kromkamp JC, Zuur AE, Herman PMJ (2014) Reproductive phenology of coastal marine bivalves in a seasonal environment. J Plankton Res 36:1512–1527

Phillips NE (2007) High variability in egg size and energetic content among intertidal mussels. Biol Bull (Woods Hole) 212:12–19

Pollack JB, Kim HC, Morgan EK, Montagna PA (2011) Role of flood disturbance in natural oyster (*Crassostrea virginica*) population maintenance in an estuary in south Texas, USA. Estuaries Coasts 34:187–197

Powell EN, Klinck JM, Hofmann EE, Wilson-Ormond EA, Ellis MS (1995) Modeling oyster populations V. Declining phytoplankton stocks and the population dynamics of American oyster (*Crassostrea virginica*) populations. Fish Res 24:199–222

Powell EN, Bochenek EA, Klinck JM, Hofmann EE (2002) Influence of food quality and quantity on the growth and development of *Crassostrea gigas* larvae: a modeling approach. Aquaculture 210:89–117

Powell EN, Klinck JM, Hofmann EE, McManus MA (2003) Influence of water allocation and freshwater inflow on oyster production: a hydrodynamic–oyster population model for Galveston Bay, Texas, USA. Environ Manage 31:100–121

Powell EN, Bochenek EA, Klinck JM, Hofmann EE (2004) Influence of short-term variations in food on survival of *Crassostrea gigas* larvae: a modeling study. J Mar Res 62: 117–152

Powell EN, Morson J, Klinck JM (2011) Application of a gene-based population dynamics model to the optimal egg size problem: Why do bivalve planktotrophic eggs vary in size? J Shellfish Res 30:403–423

Powell EN, Kreeger DA, Morson JM, Haidvogel DB, Wang Z, Thomas R, Gius JE (2012) Oyster food supply in Delaware Bay: estimation from a hydrodynamic model and interaction with the oyster population. J Mar Res 70: 469–503

Powell EN, Hofmann EE, Klinck JM (2018) Oysters, sustainability, management models, and the world of reference points. J Shellfish Res 37:833–849

Powers SP, Grabowski JH, Roman H, Geggel A, Rouhani S, Oehrig J, Baker M (2017) Consequences of large-scale salinity alteration during the *Deepwater Horizon* oil spill on subtidal oyster populations. Mar Ecol Prog Ser 576: 175–187

Provenzano AJ Jr (1961) Effects of the flatworm *Stylochus ellipticus* (Girard) on oyster spat in two salt water ponds in Massachusetts. Proc Natl Shellfish Assoc 50:83–88

Pruett JL, Showalter Otts S, Willett KL, Fairbanks L, Darnell KM, Gochfeld DJ (2024) A past, present, and future outlook on the Mississippi oyster fishery. J Shellfish Res 43: 1–13

Prytherch HF (1929) Investigation of the physical conditions controlling spawning of oysters and the occurrence, distribution, and setting of oyster larvae in Milford Harbor, Connecticut. Bull Bur Fish 44:429–503

Przeslawski R, Bourdeau PE, Doall MH, Pan J, Perino L, Padilla DK (2008) The effects of a harmful alga on bivalve larval lipid stores. Harmful Algae 7:802–807

R Core Team (2023) R: a language and environment for statistical computing. R Foundation for Statistical Computing, Vienna

Rhodes EW, Landers WS (1973) Growth of oyster larvae, *Crassostrea virginica*, of various sizes in different concentrations of the chrysophyte, *Isochrysis galbana.* Proc Natl Shellfish Assoc 63:53–59

Rico-Villa B, Pouvreau S, Robert R (2009) Influence of food density and temperature on ingestion, growth and settlement of Pacific oyster larvae, *Crassostrea gigas.* Aquaculture 287:395–401

Riekenberg J, Bargu S, Twiley R (2015) Phytoplankton community shifts and harmful algae presence in a diversion influenced estuary. Estuaries Coasts 38:2213–2226

Roelke D, Li H, Hayden N, Miller C, Davis S, Quigg A, Buyukates Y (2013) Co-occurring and opposing freshwater inflow effects on phytoplankton biomass, productivity and community composition of Galveston Bay, USA. Mar Ecol Prog Ser 477:61–76

Romberger HP, Epifanio CE (1981) Comparative effects of diets consisting of one or two algal species upon assimilation efficiencies and growth of juvenile oysters, *Crassostrea virginica* (Gmelin). Aquaculture 25:77–87

Rothschild BJ, Ault JS, Goulletquer P, Héral M (1994) Decline of the Chesapeake Bay oyster population: a century of habitat destruction and overfishing. Mar Ecol Prog Ser 111:29–39

Scharping RJ, Plough LV, Meritt DW, North EW (2019) Low-salinity tolerance of early-stage oyster larvae from a mesohaline estuary. Mar Ecol Prog Ser 613:97–106

Schlesselman GW (1955) The Gulf Coast oyster industry of the United States. Geogr Rev 45:531–541

Schmider E, Ziegler M, Danay E, Beyer L, Bühner M (2010) Is it really robust? Methodology (Gött) 6:147–151

Seitzinger SP, Sanders RW, Styles R (2002) Bioavailability of DON from natural and anthropogenic sources to estuarine plankton. Limnol Oceanogr 47:353–366

Shumway S (1996) Natural environmental factors. In: Kennedy VS, Newell RIE, Eble AF (eds) The eastern oyster, *Crassostrea virginica*. Maryland Sea Grant, College Park, MD, p 467–515

Solinger LK, Ashton-Alcox KA, Powell EN, Hemeon KM, Pace SM, Soniat TM, Poussard LM (2022) Oysters beget shell and vice versa: generating management goals for live oysters and the associated reef to promote maximum sustainable yield of *Crassostrea virginica.* Can J Fish Aquat Sci 79:1241–1254

Soniat TM, Ray SM (1985) Relationships between possible available food and the composition, condition and reproductive state of oysters from Galveston Bay, Texas. Contrib Mar Sci 28:109–121

Soniat TM, Ray SM, Jeffrey LM (1984) Components of the seston and possible available food for oysters in Galveston Bay, Texas. Contrib Mar Sci 27:127–141

Soniat TM, Powell EN, Hofmann EE, Klinck JM (1998) Understanding the success and failure of oyster populations: the importance of sampled variables and sample timing. J Shellfish Res 17:1149–1165

Soniat TM, Conzelmann CP, Byrd JD, Roszell DP, Bridevaux JL, Suir KJ, Colley SB (2013) Predicting the effects of proposed Mississippi River diversions on oyster habitat quality; application of an oyster habitat suitability index model. J Shellfish Res 32:629–638

Soniat TM, Powell EN, Cooper NA, Pace SM, Solinger LK (2021) Predicting oyster harvests at maximum sustained yield: application of cultch and stock benchmarks to depleted public oyster reefs in the northern Gulf of Mexico. J Shellfish Res 40:429–449

Talmage SC, Gobler CJ (2009) The effect of elevated carbon dioxide concentrations on the metamorphosis, size, and survival of larval hard clams (*Mercenaria mercenaria*), bay scallops (*Argopecten irradians*), and eastern oysters (*Crassostrea virginica*). Limnol Oceanogr 54:2072–2080

Thompson PA, Harrison PJ (1992) Effects of monospecific algal diets of varying biochemical composition on the growth and survival of Pacific oyster (*Crassostrea gigas*) larvae. Mar Biol 113:645–654

Thompson PA, Guo X, Harrison PJ (1996) Nutritional value of diets that vary in fatty acid composition for larval Pacific oysters (*Crassostrea gigas*). Aquaculture 143:379–391

Turner RE (2006) Will lowering estuarine salinity increase Gulf of Mexico oyster landings? Estuaries Coasts 29:345–352

Utting SD (1986) A preliminary study on growth of *Crassostrea gigas* larvae and spat in relation to dietary protein. Aquaculture 56:123–138

Wikfors GH, Twarog JW, Ukeles R (1984) Influence of chemical composition of algal food sources on growth of juvenile oysters, *Crassostrea virginica.* Biol Bull (Woods Hole) 167:251–263

Wilson-Ormond EA, Powell EN, Ray SM (1997) Short-term and small-scale variation in food availability to natural oyster populations: food, flow and flux. Mar Ecol 18:1–34

Zhang S, Long LJ, Zhou YC, Yin H, Xiao Z, Chen YF (2010) Effects of glycopeptides on development, growth and non-specific immunity of pearl oyster *Pinctada fucata* (Gould). Aquacult Nutr 16:520–527

zu Ermgassen PSE, Spalding MD, Grizzle RE, Brumbaugh RD (2013) Quantifying the loss of a marine ecosystem service: filtration by the eastern oyster in US estuaries. Estuaries Coasts 36:36–43

Editorial responsibility: James McClintock, Birmingham, Alabama, USA
Reviewed by: 3 anonymous referees

Submitted: January 22, 2024
Accepted: August 1, 2024
Proofs received from author(s): September 14, 2024